DNA-triggered innate immune responses are propagated by gap junction communication

Suraj J. Patel[a,b,c,1], Kevin R. King[a,b,c,1], Monica Casali[a,c], and Martin L. Yarmush[a,b,c,2]

[a]Department of Surgery, Center for Engineering in Medicine, Massachusetts General Hospital, Boston, MA 02114; [b]Division of Health, Sciences, and Technology, Massachusetts Institute of Technology, Harvard Medical School, Cambridge, MA 02139; and [c]Shriners Hospital for Children, Boston, MA 02114

Cells respond to infection by sensing pathogens and communicating danger signals to noninfected neighbors; however, little is known about this complex spatiotemporal process. Here we show that activation of the innate immune system by double-stranded DNA (dsDNA) triggers intercellular communication through a gap junction-dependent signaling pathway, recruiting colonies of cells to collectively secrete antiviral and inflammatory cytokines for the propagation of danger signals across the tissue at large. By using live-cell imaging of a stable IRF3-sensitive GFP reporter, we demonstrate that dsDNA sensing leads to multicellular colonies of IRF3-activated cells that express the majority of secreted cytokines, including IFNβ and TNFα. Inhibiting gap junctions decreases dsDNA-induced IRF3 activation, cytokine production, and the resulting tissue-wide antiviral state, indicating that this immune response propagation pathway lies upstream of the paracrine action of secreted cytokines and may represent a host-derived mechanism for evading viral antiinterferon strategies.

innate immunity | IRF | TLR | interferon

The ability of the innate immune system to propagate antiviral and inflammatory signals from the local cellular microenvironment to the tissue at large is critical for survival (1). At the onset of a viral infection, individual cells sense invading pathogens and elicit innate immune responses that spread from infected to uninfected cells, establishing an overall antiviral state (2). Secreted cytokines such as interferon β (IFNβ) and tumor necrosis factor (TNFα) are 2 key mediators of these responses (3). To evade the host immune system, viruses have evolved strategies for limiting the secretion of these cytokines (4). Nevertheless, the immune system remains capable of clearing many viral pathogens, suggesting that the host may have subsequently evolved additional mechanisms for propagating antiviral and inflammatory signals, beyond the paracrine action of cytokines (5).

The innate immune system uses pathogen-recognition receptors to sense nucleic acids during infection or tissue damage (6). Pathogen-derived nucleic acids generate potent immune responses, as they are not typically found in a host cell or in particular intracellular locations (7, 8). Several receptors have been identified for their ability to recognize viral RNA, and their mechanistic details have been well studied (8). In contrast, the sensing of viral DNA and the subsequent triggering of a host antiviral response remain poorly understood. Double-stranded DNA (dsDNA) derived from host, viral, or synthetic sources elicits a potent immune response by activating a TLR-independent cytosolic DNA sensor (9, 10), such as the recently identified DNA-dependent activator of IFN regulatory factors (DAI) (11). The TLR-independent pathway for dsDNA sensing activates TBK1 and IKKε for the phosphorylation of transcription factor IRF3, which binds to IFN-sensitive response element (ISRE) sequences, triggering the robust production of type I interferons such as IFNβ (9, 12, 13). In addition to IFNβ, a successful antiviral response requires the establishment of an inflammatory state through cytokines such as TNFα (14). The secretion of IFNβ and TNFα is thought to play an important role in propagating antiviral innate immune responses from individual infected cells to noninfected neighbors, priming them to resist the spread of infection (14). However, although this communication is commonly attributed to secreted cytokines, the spatiotemporal details remain speculative, and the possibility of contact-mediated communication unexplored.

Cell–cell communication can be categorized by its dependency on contact. Contact-independent signaling is ideal for long-range communication whereas contact-dependent signaling is best suited for spatially localized rapid communication (15). Gap junction intercellular communication represents an important class of contact-dependent signaling. Gap junctions are assemblies of intercellular channels composed of connexin (Cx) proteins organized into 2 subsets, alpha connexins (e.g., Cx43) and beta connexins (e.g., Cx32, Cx26). Connexins from each subset oligomerize to form a hemichannel. A functional channel is formed when a hemichannel from one subset assembles with a hemichannel of the same subset from an adjacent cell (16). The resulting gap junctions directly connect the cytosol of the coupled cells, allowing the exchange of ions, nutrients, and secondary messengers for the maintenance of tissue homeostasis (17). In the context of innate immunity, gap junction communication has been shown to be regulated by pathogen associated stimuli such as LPS and peptidoglycans, and secreted proinflammatory cytokines such as TNFα, IL1β, and IFNγ (18, 19). However, the relative contributions of contact-dependent and contact-independent communication in the establishment of host defenses have not been explored.

Given the incomplete understanding of host innate immune response propagation, we used a stable ISRE-GFP monoclonal reporter to explore the spatiotemporal patterns of IRF3 activation in response to dsDNA stimulation and investigated the intercellular signaling pathways between infected and noninfected cells for establishing an antiviral state. We found that dsDNA stimulation induced spatially heterogeneous responses characterized by the formation of multicellular colonies of IRF3 activated cells that collectively expressed more than 95% of critical secreted cytokines, including IFNβ and TNFα. Functional gap junctions were necessary for the formation of these IRF3 active colonies and blocking gap junctions with genetic specificity limited the secretion of IFNβ and TNFα and the corresponding antiviral state. Our findings describe a previously unknown intercellular signaling pathway triggered by cytosolic dsDNA sensing and provide evidence that gap junction communication is critical for the amplification of antiviral and inflammatory responses, prior to paracrine-mediated propagation by cytokines.

IMMUNOLOGY

Fig. 1. Stable ISRE reporters reveal dsDNA-induced spatiotemporal patterns. (*A*) ISRE-GFP reporter cell line was created to study dsDNA-induced responses in living cells. (*B*) Percentage of GFP-positive reporter cells measured by flow cytometry after 24-h stimulation with dsRED, poly(A:T), poly(I:C), OptiMEM, Lipofectamine, CpG-ODN, IFNβ, LPS, ssDNA [Poly(A)], and siRNA. (*C*) Reporter expression of IFNβ and TNFα measured by qPCR after 12-h stimulation with 4 μg/mL poly(A:T). (*D*) Flow-cytometry distribution of ISRE reporter fluorescence 24 h after exposure to poly(A:T). (*E*) Percentage of GFP-positive reporter cells measured by flow cytometry after 24-h stimulation with an increasing dose of poly(A:T). (*F* and *G*) Representative 5× (scale bar ≈200 μm) (*F*) and 16× (scale bar ≈120 μm) (*G*) fluorescence images of reporters stimulated with various doses of poly(AT) for 24 h. (*H* and *I*) Fluorescence time-lapse microscopy of poly(A:T)-stimulated reporters (*H*) with a corresponding phase image of the confluent monolayer at 15 h (scale bars ≈200 μm) (*I*). (*J*) Contour maps outlining automated colony identification at each time point. (*K*) Identification of dsDNA-sensing cells within ISRE-GFP colonies. ISRE-GFP reporters were stimulated with 2 μg/mL of complexed dsRED DNA and imaged 24 h later by fluorescence microscopy. Representative fluorescence image of ISRE-GFP colony, with identification of dsRED DNA-sensing cell.

Results

GFP Reporters Sensitive and Specific for IRF3-Activating Stimuli.

dsDNA is known to stimulate the expression of genes with ISRE consensus sequences in their promoters through activation of the IRF3 transcription factor (9, 12). To investigate the spatiotemporal evolution of dsDNA-induced gene expression, we created a stable monoclonal ISRE-GFP reporter cell line in a hepatocyte-derived H35 cell line and selected clones exhibiting low-baseline GFP expression in the absence of stimuli and high dsDNA-induced GFP expression (Fig. 1*A*). To characterize the reporter, we first assessed its specificity for IRF3-dependent gene expression by exposing confluent reporter monolayers to various immunostimulatory molecules and measuring ISRE reporter fluorescence by using flow cytometry (Fig. 1*B*). When reporters were exposed to synthetic B-form Poly(dA-dT):Poly(dA-dT) (hereafter referred to as dsDNA) or DNA encoding the red fluorescent protein (dsRED), total population fluorescence increased in a dose-dependent fashion. Similarly, when cells were stimulated with polyinosinic:polycytidylic acid [poly(I:C)], a synthetic double-stranded RNA known to activate IRF3, dose-dependent increases in total fluorescence were also observed. In contrast, IRF3-independent stimuli such as TLR9-dependent CpG DNA, IFNβ, poly(A) ssDNA, and siRNA did not elicit measurable increases in ISRE reporter fluorescence at any of the doses examined. As anticipated, LPS, which classically signals through TLR4 and IRF3, failed to activate the ISRE reporter, consistent with the fact that nonimmune cells do not express significant levels of TLR4 (confirmed by qPCR). To verify that the ISRE reporters retained previously reported dsDNA-induced responses (9), we confirmed the expression of IFNβ and TNFα after 12 h of dsDNA stimulation (Fig. 1*C*). Taken together, these results demonstrate that the ISRE reporters are sensitive for

both dsDNA and Poly(I:C) stimulation, and specific for IRF3-activating stimuli.

When we examined the distribution of ISRE reporter fluorescence after dsDNA stimulation by flow cytometry, we found that increasing doses of dsDNA resulted in increasing numbers of activated cells rather than increasing levels of activation in all cells, indicating that the cellular response was heterogeneous (Fig. 1 *D* and *E*). Therefore, we used fluorescence microscopy to examine the distribution of dsDNA-induced GFP expression and discovered a striking spatial pattern. dsDNA stimulation of confluent reporter monolayers exhibited well-delineated clusters of GFP-positive cells or "colonies" in an otherwise dark background of nonactivated cells. Increasing doses of dsDNA led to increasing numbers of colonies with eventual bridging of adjacent colonies (Fig. 1 *F* and *G*). To gain further insight into colony formation, we examined the temporal evolution of ISRE-activated colonies by monitoring GFP-reporter induction with time-lapse fluorescence microscopy and quantifying colony area by using custom automated image analysis software (Fig. 1 *H* and *J*) (see Movie S1 online). Colony activation began 8–12 h after dsDNA stimulation and grew to a steady-state size with clearly demarcated colony borders characterized by highly induced reporter cells inside and uninduced cells outside. These findings confirm that dsDNA stimulation leads to spatially heterogeneous patterns of ISRE-activated colonies in an otherwise uninduced confluent monolayer of cells. Interestingly, Poly(I:C) stimulation also led to ISRE reporter activation; however, the response was spatially homogeneous across the reporter monolayer and did not result in colony formation.

Because dsDNA requires polyelectrolyte complexing for immunogenicity and high molecular weight complexes have short diffusion distances, we reasoned that dsDNA complexes land in discrete

Fig. 2. Spatial gene profiling triggered by dsDNA stimulation. (A) ISRE-GFP reporter cells were stimulated with 4 μg/mL dsDNA for 12 h and then sorted by FACS into GFP-positive and GFP-negative cells. (B) Expression of IFNβ, TNFα, and IP10 in GFP-sorted (positive and negative) and -unsorted cells, as assessed by qPCR. (C) Expression of IFNβ-mediated antiviral genes, PKR, and OAS1. Data were normalized to control mock dsDNA-stimulated cells.

locations within the cultured monolayer, stimulate individual dsDNA-sensing cells, and ISRE colony formation arises by a secondary intercellular communication signal. To clarify which cells were directly and indirectly activated by dsDNA, ISRE reporters were stimulated with dsRED. dsRED stimulation of ISRE-GFP reporters resulted in multicellular ISRE reporter cell colonies surrounding individual dsRED DNA-sensing cells (Fig. 1K and Fig. S1). By using the custom automated image analysis software discussed above, we determined that the average colony was comprised of 23.5 ISRE-activated cells, of which 2.3 cells were dsRED DNA-sensing cells (see Fig. S1D).

Spatiotemporal IRF3-Mediated Gene Expression. We next sought to determine whether the colonies of GFP⁺ ISRE reporters had functional significance by examining their gene expression profiles and comparing them with their GFP⁻ neighbors. Confluent monolayers of reporters were stimulated with dsDNA for 12 h, sorted into GFP⁺ and GFP⁻ populations by FACS, and examined for expression of IRF3-mediated genes by qPCR (Fig. 2A). GFP⁺ cells represented less than 8% of the total population, yet expressed more than 95% of secreted cytokines and chemokines including IFNβ, TNFα, and IP10 (Fig. 2B). In contrast, expression of IFNβ-inducible genes, with direct antiviral properties such as PKR

and OAS1, did not differ significantly between the 2 populations (Fig. 2C). Given the commonly held view that antiviral genes are expressed in response to the paracrine action of IFNβ, these results suggest that dsDNA-sensing in individual cells leads to IRF3 activation in colonies of cells that collectively secrete cytokines, such as IFNβ and TNFα, to establish an antiviral state across the broader population.

IRF3 Activation by Contact-Dependent Intercellular Communication. We hypothesized that IRF3-activated colony formation required secondary intercellular communication from dsDNA-sensing cells. To test this hypothesis, we developed a transplant coculture system using dsDNA-stimulated nonreporter cells as donors and unstimulated ISRE reporters as recipients. Donor cells were stimulated with dsDNA for 6 h, trypsinized, thoroughly washed, and transplanted onto recipient ISRE reporters that had never been exposed to dsDNA (Fig. 3A). After 18 h of coculture, ISRE reporters were activated in small colonies surrounding donor cells (Fig. 3 B and C). In contrast, no IRF3 activity was observed in the reporters when mock dsDNA stimulated nonreporter cells were transplanted (Fig. 3C). Interestingly, not all dsDNA-stimulated cells were able to activate IRF3 in neighboring reporters. dsDNA-stimulated human cervical cancer cells (HeLa) and mouse neuroblastoma cells (N2A) were unable to activate IRF3 in the reporters (Fig. 3 B and C), demonstrating that the phenomenon is cell-type specific and not an artifact of nonspecific dsDNA carry-over from the donor cells. Donor cells were also stimulated with dsRED DNA, to identify them within the coculture, and to confirm that they make contact and adhere to the reporter cells (see Fig. S4). To investigate whether direct cell contact was necessary for this dsDNA-induced secondary intercellular communication, we cultured dsDNA-stimulated donors and ISRE reporter recipients on opposite surfaces of a microfluidic parallel plate bioreactor (separation gap of ≈50 μm; see Fig. S5). Negligible reporter induction was observed, suggesting that dsDNA-induced intercellular communication is contact dependent. Taken together, these data suggest that dsDNA stimulation induces contact-dependent intercellular communication from dsDNA-sensing cells to their unstimulated neighbors, propagating an IRF3-activating signal and amplifying IRF3-dependent gene expression.

To further clarify the pathways connecting donor dsDNA-sensing and recipient IRF3 activation, we used genetic knockout mouse embryonic fibroblasts (MEFs) to determine the necessity of critical proteins. Wild-type MEF donors stimulated with dsDNA activated ISRE in reporter recipients (Fig. 3 D and E). In addition, MEFs deficient in both TBK1 and IKKε (Tbk1⁻/⁻Ikbke⁻/⁻), kinases necessary for IRF3 activation, also activated ISRE in reporter cells (Fig. 3 D and E). Similarly, dsDNA-stimulated MEFs
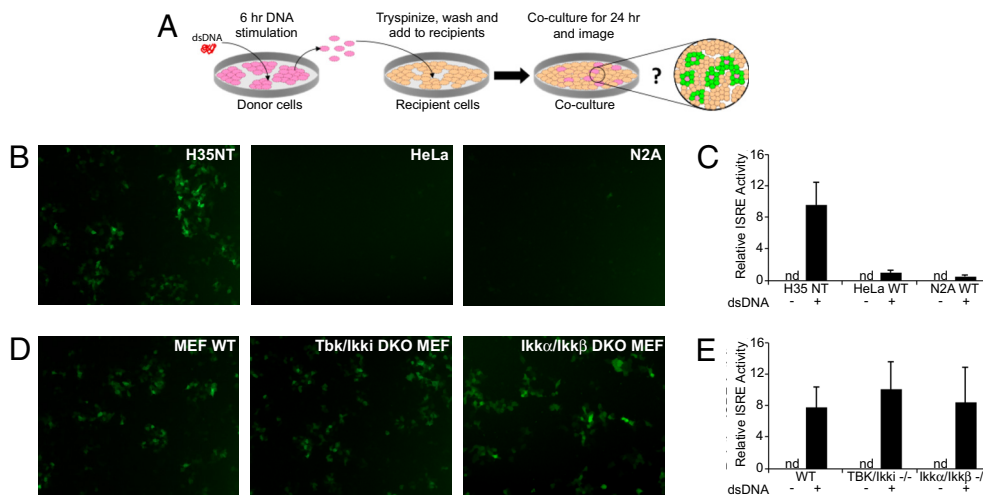
Fig. 3. IRF3-activated colonies form by contact-dependent cell–cell communication. (A) Transplant coculture system schematic. Non-ISRE reporter donor cells were stimulated with 10 μg/mL dsDNA for 6 h. The donors were washed and trypsinized, and a subpopulation was cocultured with ISRE-GFP reporter recipient cells. The coculture was assayed 18 h later by fluorescence microscopy and flow cytometry. (B and D) Representative 10× fluorescence images of reporter recipient cells cocultured with various dsDNA-stimulated donor cells. (C and E) Relative GFP activity quantified by flow cytometry.
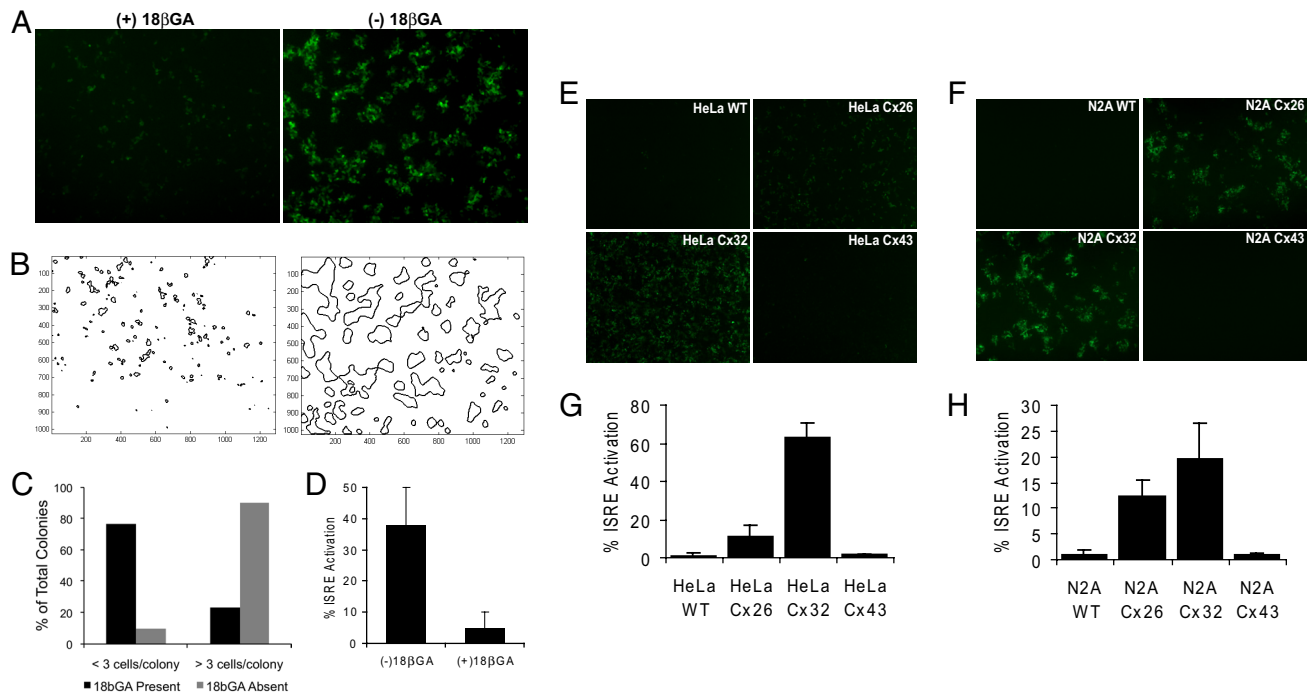
Fig. 4. dsDNA-induced IRF3 amplification requires gap junctions. (*A*) ISRE-GFP reporters were stimulated with 4 μg/mL dsDNA, and GFP activity was assayed 18 h later. (*A* and *B*) Representative 5× fluorescence images of dsDNA-stimulated GFP reporters (*A*) and corresponding contour maps outlining automated colony identification (*B*), in the presence (left) or absence (right) of 25 μM 18βGA. (*C*) Percentage of dsDNA-induced colonies less than 3 cells and more than 3 cells, in the presence (black) or absence (gray) of 18βGA. (*D*) dsDNA-stimulated ISRE-GFP reporter activity with or without 18βGA treatment, as determined by FACS. (*E*–*H*) Transplant coculture experiments with genetically modified cells. Donor HeLa or N2A cells (WT, Cx26-expressing, Cx32-expressing, or Cx43-expressing) were stimulated with 10 μg/mL dsDNA for 6 h and then transplanted onto recipient ISRE-GFP reporters for 18 h. (*E*) Representative 5× fluorescence images of dsDNA-stimulated HeLa WT, HeLa Cx26, HeLa Cx32, and HeLa Cx43 cells cocultured with GFP reporters. (*F*) Representative 5× fluorescence images of dsDNA-stimulated N2A WT, N2A Cx26, N2A Cx32, and N2A Cx43 cells cocultured with GFP reporters. (*G*) ISRE-GFP activity in HeLa/reporter cocultures, as determined by FACS. (*H*) ISRE-GFP activity in N2A/reporter cocultures, as determined by FACS.

deficient in both IKKα and IKKβ (IKKα$^{-/-}$IKKβ$^{-/-}$), kinases essential for NFκB activation, also activated ISRE in reporter cells (Fig. 3 *D* and *E*). MEFs deficient in both MyD88 and TRIF (MyD88$^{-/-}$TRIF$^{-/-}$) were also able to activate ISRE reporter recipients. Together, these data suggest that dsDNA-induced intercellular communication is TLR-independent and occurs upstream of both IRF3 and NFκB activation in dsDNA sensing cells.

Gap Junctions Are Necessary for Amplified IRF3 Activation. Gap junction communication enables the rapid, localized exchange of information between cells linked through connexin protein channels (16). To determine the necessity of gap junctions in the dsDNA-induced intercellular communication, we pretreated ISRE reporters with 18β-glycyrrhetinic acid (18βGA), a molecular inhibitor of gap junctions (20), before dsDNA stimulation. Compared with vehicle controls, pretreatment with 18βGA dramatically reduced colony size, resulting in mostly single cell reporter activation (Fig. 4*A*). Images were quantified by creating isointensity contour maps and calculating the average size per colony for each colony present in the images (Fig. 4*B*). The average size of dsDNA-induced ISRE-activated colonies was reduced by more than 10-fold with 18βGA treatment compared with no 18βGA treatment. More than 75% of all colonies formed in the presence of 18βGA contained fewer than 3 cells, whereas more than 90% of all colonies formed in the absence 18βGA contained more than 3 cells (Fig. 4*C*). In addition, the overall number of ISRE-activated GFP-positive cells was decreased from 38% to 5%, as a result of gap junction blockage (Fig. 4*D*). These results were further validated by Cx32 knockdown analysis using Cx32-targeted siRNA (see Fig. S3). Compared with control siRNA, Cx32 siRNA knockdown resulted in a significant decrease in both the size of dsDNA-induced ISRE active colonies

and in the overall number of dsDNA-induced GFP-positive reporters. More than 70% of all colonies formed in the presence of Cx32 knockdown contained fewer than 3 cells, whereas more than 85% of all colonies formed in the presence of control knockdown contained more than 3 cells (see Fig. S3).

The utility of chemical gap junction inhibitors such as 18βGA is limited because of their nonspecific side effects and unknown mechanism of action (21). Therefore, to definitively demonstrate the necessity of gap junction communication for the propagation of IRF3 activity, we used the transplant coculture system with genetically modified cell lines. HeLa and N2A cell lines have been historically shown to be gap junction- and connexin-deficient (21, 22). We obtained modified monoclonal HeLa and N2A cells stably transfected with individual connexin transgenes (Cx26, Cx32, or Cx43), thereby reconstituting connexin expression and gap junction communication (21, 22). PCR analysis was performed to verify appropriate connexin expression in all HeLa and N2A cells. PCR analysis showed that ISRE reporters express only Cx32 of the β-subset and therefore only form functional gap junction channels with other cells expressing β connexins 26 or 32. When WT and Cx43-expressing HeLa and N2A cells were stimulated with dsDNA, minimal ISRE reporter activation was measured (HeLa WT, 0.5%; N2A WT, 1.0%; HeLa Cx43, 2%; N2A Cx43, 1.5%), suggesting a lack of intercellular communication (Fig. 4 *E*–*H*). However, when Cx26- and Cx32-expressing cells were stimulated with dsDNA, significant ISRE reporter activation was observed (Fig. 4 *E* and *F*), with 63% of reporters activated by Cx32-expressing HeLa cells and 23% by Cx32-expressing N2A cells (Fig. 4 *G* and *H*). These data suggest that functional gap junction channels are necessary for dsDNA-induced intercellular communication and for amplifying IRF3 activation. To further generalize the utility of gap junctions for
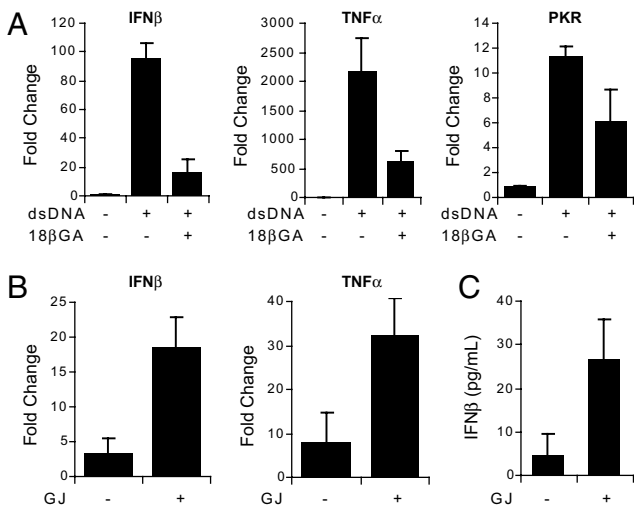
Fig. 5. Gap junction communication results in propagation of antiviral and inflammatory signals in response to dsDNA stimulation. (*A*) ISRE-GFP reporter cells were stimulated with 4 μg/mL dsDNA for 8 h in the presence or absence of 18βGA. Expression of IFNβ, TNFα, and PKR was assessed by quantitative RT-PCR. (*B* and *C*) Reporter cells (of rat lineage) expressing only Cx32 were stimulated with 10 μg/mL dsDNA for 6 h and then cocultured with unstimulated gap junction-deficient (HeLa WT) or gap junction-expressing (HeLa Cx32) human HeLa cells. (*B*) After 10 h of coculture, HeLa cells were analyzed by quantitative RT-PCR for IFNβ and TNFα expression using human-specific PCR primers. (*C*) ELISA for human IFNβ, secreted into coculture supernatants by HeLa cells after 24 h. dsDNA-stimulated reporter coculture with HeLa WT is indicated as GJ −, and coculture with HeLa Cx32 is indicated as GJ +.

amplifying IRF3 activation in other cell types, we constructed another ISRE-GFP reporter in a stromal hepatic stellate cell line (HSC). When the HSC ISRE-GFP reporters were stimulated with dsDNA, they were able to form multicellular colonies of IRF3-activated reporters in a gap junction-dependent manner (see Fig. S2).

Propagation of Antiviral and Inflammatory Responses by Gap Junctions. To investigate the physiological significance of gap junction-mediated amplification of IRF3 activity, we disrupted gap junctions and examined the ability of cells to mount innate immune responses. When ISRE reporters were pretreated with 18βGA and stimulated with dsDNA, they expressed significantly lower levels of critical antiviral cytokines in comparison to vehicle pretreatment. After 8 h of dsDNA stimulation, 18βGA pretreated cells expressed 6-fold less IFNβ than vehicle-treated cells (Fig. 5*A*). Expression of the IFNβ-stimulated antiviral protein PKR was also significantly reduced by 2-fold ($P < 0.05$) in the 18βGA-treated cells, compared with vehicle treatment (Fig. 5*A*). Similarly, the expression of the proinflammatory cytokine, TNFα, was reduced by 3.5-fold with gap junction inhibition (Fig. 5*A*).

We further verified the role of gap junctions in innate immune responses by using genetically modified cells and the transplant coculture system described above. Rat ISRE reporter cells, which express only Cx32, were stimulated with dsDNA and then cocultured with unstimulated human HeLa cells that either lacked gap junctions (HeLa WT) or expressed Cx32 gap junctions (HeLa Cx32). Recipient HeLa cells were then analyzed for cytokine expression and secretion using human-specific PCR primers and ELISAs. When dsDNA-stimulated reporter cells were cocultured with HeLa Cx32 cells, HeLa IFNβ and TNFα expression was increased by 6- and 4-fold respectively, compared to coculture with gap junction-deficient HeLa WT cells (Fig. 5*B*). Additionally, coculture of dsDNA-stimulated reporters with HeLa Cx32 cells triggered a 5-fold increase in production of human IFNβ compared to coculture with gap junction-deficient HeLa WT cells (Fig. 5*C*). Taken together, these data suggest that gap junctions amplify

dsDNA-induced expression and secretion of IFNβ and TNFα, and that without functional gap junctions, cytokine secretion is impaired, consequently reducing the antiviral state in the overall population.

Discussion

Investigations of innate immune response propagation have typically focused on the paracrine action of secreted cytokines (23). Here we provide evidence that gap junctions amplify innate immune responses triggered by cytosolic dsDNA. Using a stable monoclonal GFP reporter cell line that is sensitive and specific for IRF3-mediated gene expression, we visualized the spatiotemporal evolution of IRF3 activity in response to dsDNA stimulation. Sorting these cells by GFP activity, we demonstrated that dsDNA stimulation of confluent cell monolayers leads to the formation of 2 distinct cell populations, each with a unique gene expression program. The IRF3-active subpopulation was spatially arranged in multicellular colonies that collectively served as the dominant source of diffusible cytokines for the establishment of an overall antiviral state. These colonies were formed by gap junction-dependent communication between dsDNA-stimulated cells and their unstimulated neighbors. In the absence of gap junctions, IRF3-activated colonies and total cytokine secretion were significantly diminished, as was the resulting antiviral state. These findings place contact-dependent communication upstream of secreted cytokines, at the earliest stages of dsDNA-induced antiviral and inflammatory responses, and they offer gap junction communication as a mechanism for amplifying dsDNA-mediated innate immunity.

Gap junctions are networks of intercellular communication channels that allow local cell populations to rapidly share and spread signals (16). This work has identified a gap junction-dependent "recruitment" process whereby infected cells engage surrounding noninfected cells to secrete cytokines. The molecular details of this process, its mediator, its regulation, and the pathways that lead to its generation remain unclear, and further investigation is necessary. Many common gap junction communication mediators such as Ca^{2+}, cAMP, and IP3 have been implicated in the activation of inflammatory transcription factors (24, 25). For example, calcium fluxes have been shown to activate transcription factors such as NFκB and AP1, resulting in the expression of proinflammatory cytokines (24). Although there are links connecting gap junction communication and inflammation, our results represent the first connection to antiviral responses.

Secreted cytokines such as IFNβ and TNFα are known to mediate the spread of antiviral and inflammatory signals for the protection of noninfected cells against subsequent attack (3). However, at the earliest stages of an infection when only a limited number of cells have been exposed to the pathogen, recruitment of neighboring noninfected cells and amplification of cytokine production is particularly important. Paracrine feed-forward loops have been proposed to increase the number of cytokine secreting cells beyond those initially infected; however, their significance is unclear (23). For example, dsDNA stimulation of type I IFN receptor-deficient macrophages induced similar IFNβ expression compared with wild-type controls, suggesting that the IFNβ paracrine loops may not be necessary for amplifying IFNβ secretion (10). In this work, we show that gap junction communication provides a mechanism for single infected cells to recruit their neighbors and amplify cytokine production prior to the activation of paracrine loops. Compared with secreted cytokine amplification, gap junction-mediated signaling is typically faster and therefore better suited for anticipating and preventing the rapid spread of an invading pathogen (16).

Although the existence of dsDNA-stimulated intercellular communication is clear, the precise signaling pathway remains unknown. Evidence from transplant coculture experiments showed that communication does not require MyD88 or TRIF, thereby eliminating the necessity of all known TLR pathways. Additionally, the communication was independent of TBK1, IKKε, IKKα and IKKβ in the dsDNA sensing cell, demonstrating that signal gener-

ation and transmission occur upstream of dsDNA-induced activation of NFκB- and IRF3-associated kinases. A recently identified dsDNA-sensing molecule, DAI, was shown to bind TBK1 and IRF3, thereby facilitating IRF3 phosphorylation and activation (11). Interestingly, we found that IRF3 can be activated in cells that were never directly exposed to dsDNA. Instead, these cells only required contact with dsDNA-stimulated cells expressing compatible connexins. Because the dsDNA used in these experiments (≈400bp) is too large to pass through gap junctions (21), our results point to a unique mechanism for activating TBK1- or IKKε-mediated phosphorylation of IRF3.

Viruses have evolved numerous strategies for silencing the defenses of infected cells. Many viruses prevent infected cells from propagating "danger signals" by inhibiting IRF3-mediated production and secretion of antiviral cytokines such as IFNβ (4, 5). In addition to suppressing antiviral signals, dsDNA viruses such as vaccinia virus, also inhibit host proinflammatory signaling by inhibiting the activation of NFκB and limiting the secretion of TNFα and IL1β (26). This work demonstrated that gap junctions enable the rapid local spread of dsDNA-induced IRF3-activating signals from infected cells to their noninfected neighbors, potentially allowing the escape of host danger signals before the virus has time to disable the antiviral program in the infected cell. This type of immediate response has the advantage of rapidly mobilizing host defenses against infection, resulting in the early secretion of large amounts of cytokines for broadly inducing an antiviral state. Indeed, we found that cells deficient in gap junctions produced significantly less IFNβ and TNFα, resulting in substantial decreases in expression of antiviral genes such as PKR. Furthermore, 2 dsDNA viruses that represent important causes of human disease, herpesvirus HSV2 and human papilloma virus HPV16, were shown to express viral proteins that close gap junctions of infected cells, suggesting that viruses have identified gap junction communication as a critical mode for host defense signaling and have begun evolving strategies to inhibit these defenses (27, 28).

Mammalian cells are exposed to cytosolic dsDNA during viral and intracellular bacterial infection, during exposure to self-DNA from dying cells, and during DNA-based gene therapy (7, 9–11, 14). The ability to increase and decrease the innate immune response in these settings would have significant potential as a clinically relevant therapeutic. In this regard, the stable monoclonal ISRE reporter represents an important experimental tool for discovering modulators of the innate immune responses to these stimuli and the intercellular communication mechanisms they use for propagation

and amplification. However, modulation of gap junction communication continues to be experimentally challenging. Genetic methods are certainly the most definitive; however, the degeneracy of connexin proteins required to form functional gap junctions is such that cells deficient in individual connexins may not show significant defects due to compensatory expression of other connexins. Future studies will be needed to evaluate the full physiologic significance of gap junction communication in augmenting responses to dsDNA-based stimuli.

Materials and Methods

Cells and Reagents. Hepatocyte-derived H35 cells were maintained as previously described (29). Construction of the ISRE-GFP reporter was performed as described in *SI Materials and Methods*. MEFs from WT and knockout mice and Cx26-, Cx32-, and Cx43-expressing HeLa and N2A cells were gifts (see *Acknowledgments*). Synthetic polydeoxynucleotides poly(dA-dT):poly(dA-dT) dsDNA and poly(dA-dT) ssDNA, synthetic poly(I:C), CpG ODN, LPS, 18β-glycyrrhetinic acid and pdsRED was purchased from commercial sources (see *SI Materials and Methods*). DNA transfections were performed by using Lipofectamine LTX (Invitrogen) at a ratio of 1.5:1 (volume/weight) with DNA as per manufacturer's protocol. For experiments involving the use of 18βGA, cells were pretreated with 25 μM 18βGA in DMEM for 1 h before dsDNA stimulation and during stimulation.

Quantitative RT-PCR and ELISA. Analysis of gene expression by quantitative RT-PCR, and protein secretion by ELISA is detailed in *SI Materials and Methods*. RT-PCR primer sequences are provided in Table S1.

Transplant Coculture Assay. Donor cells were transfected with 10 μg/mL of poly(A:T) dsDNA. Six hours after transfection, donor cells were trypsinized, washed three times in PBS, and counted. dsDNA-stimulated donor cells (1 × 10^5 cells/mL) were transplanted onto a subconfluent layer of recipient ISRE reporters, maintaining a 1:10 ratio between donor and recipient cells. After 18 h of coculture, recipient reporter cells were analyzed by fluorescent microscopy and FACS for ISRE activity. In some cases, IFNβ and TNFα secretion by recipient cells was measured by ELISA. Gene expression analysis on recipient cells was performed by quantitative RT-PCR using recipient cell species-specific primers (provided in Table S2).

1. Carter WA, De Clercq E (1974) Viral infection and host defense. *Science* 186:1172–1178.
2. Kawai T, Akira S (2006) Innate immune recognition of viral infection. *Nat Immunol* 7:131–137.
3. Hiscott J (2007) Convergence of the NF-kappaB and IRF pathways in the regulation of the innate antiviral response. *Cytokine Growth Factor Rev* 18:483–490.
4. Alcami A (2003) Viral mimicry of cytokines, chemokines and their receptors. *Nat Rev Immunol* 3:36–50.
5. Marques JT, Carthew RW (2007) A call to arms: Coevolution of animal viruses and host innate immune responses. *Trends Genet* 23:359–364.
6. Janeway Jr CA, Medzhitov R (2002) Innate immune recognition. *Annu Rev Immunol* 20:197–216.
7. Ishii KJ, Akira S (2006) Innate immune recognition of, and regulation by, DNA. *Trends Immunol* 27:525–532.
8. Kato H, et al. (2006) Differential roles of MDA5 and RIG-I helicases in the recognition of RNA viruses. *Nature* 441:101–105.
9. Ishii KJ, et al. (2006) A Toll-like receptor-independent antiviral response induced by double-stranded B-form DNA. *Nat Immunol* 7:40–48.
10. Stetson DB, Medzhitov R (2006) Recognition of cytosolic DNA activates an IRF3-dependent innate immune response. *Immunity* 24:93–103.
11. Takaoka A, et al. (2007) DAI (DLM-1/ZBP1) is a cytosolic DNA sensor and an activator of innate immune response. *Nature* 448:501–505.
12. Au WC, Moore PA, Lowther W, Juang YT, Pitha PM (1995) Identification of a member of the interferon regulatory factor family that binds to the interferon-stimulated response element and activates expression of interferon-induced genes. *Proc Natl Acad Sci USA* 92:11657–11661.
13. Grandvaux N, et al. (2002) Transcriptional profiling of interferon regulatory factor 3 target genes: Direct involvement in the regulation of interferon-stimulated genes. *J Virol* 76:5532–5539.
14. Muruve DA, et al. (2008) The inflammasome recognizes cytosolic microbial and host DNA and triggers an innate immune response. *Nature* 452:103–107.
15. Downward J (2001) The ins and outs of signalling. *Nature* 411:759–762.
16. Segretain D, Falk MM (2004) Regulation of connexin biosynthesis, assembly, gap junction formation, and removal. *Biochim Biophys Acta* 1662:3–21.
17. Goldberg GS, Valiunas V, Brink PR (2004) Selective permeability of gap junction channels. *Biochim Biophys Acta* 1662:96–101.
18. Chanson M, et al. (2001) Regulation of gap junctional communication by a proinflammatory cytokine in cystic fibrosis transmembrane conductance regulator-expressing but not cystic fibrosis airway cells. *Am J Pathol* 158:1775–1784.
19. Jara PI, Boric MP, Saez JC (1995) Leukocytes express connexin 43 after activation with lipopolysaccharide and appear to form gap junctions with endothelial cells after ischemia-reperfusion. *Proc Natl Acad Sci USA* 92:7011–7015.
20. Martin FJ, Prince AS (2008) TLR2 regulates gap junction intercellular communication in airway cells. *J Immunol* 180:4986–4993.
21. del Corsso C, et al. (2006) Transfection of mammalian cells with connexins and measurement of voltage sensitivity of their gap junctions. *Nat Protoc* 1:1799–1809.
22. Elfgang C, et al. (1995) Specific permeability and selective formation of gap junction channels in connexin-transfected HeLa cells. *J Cell Biol* 129:805–817.
23. Honda K, Takaoka A, Taniguchi T (2006) Type I interferon [corrected] gene induction by the interferon regulatory factor family of transcription factors. *Immunity* 25:349–360.
24. Dolmetsch RE, Xu K, Lewis RS (1998) Calcium oscillations increase the efficiency and specificity of gene expression. *Nature* 392:933–936.
25. Bodor J, et al. (2001) Suppression of T-cell responsiveness by inducible cAMP early repressor (ICER). *J Leukoc Biol* 69:1053–1059.
26. Deng L, Dai P, Ding W, Granstein RD, Shuman S (2006) Vaccinia virus infection attenuates innate immune responses and antigen presentation by epidermal dendritic cells. *J Virol* 80:9977–9987.
27. Fischer NO, Mbuy GN, Woodruff RI (2001) HSV-2 disrupts gap junctional intercellular communication between mammalian cells in vitro. *J Virol Methods* 91:157–166.
28. Oelze I, Kartenbeck J, Crusius K, Alonso A (1995) Human papillomavirus type 16 E5 protein affects cell-cell communication in an epithelial cell line. *J Virol* 69:4489–4494.
29. King KR, et al. (2007) A high-throughput microfluidic real-time gene expression living cell array. *Lab Chip* 7:77–85.

Unphosphorylated STAT3 accumulates in response to IL-6 and activates transcription by binding to NF κB

Jinbo Yang, Xudong Liao, Mukesh K. Agarwal, et al.

Supplemental Material	http://genesdev.cshlp.org/content/suppl/2007/10/31/gad.1553707.DC1.html
References	This article cites 54 articles, 26 of which can be accessed free at: **http://genesdev.cshlp.org/content/21/11/1396.full.html#ref-list-1**
	Article cited in: **http://genesdev.cshlp.org/content/21/11/1396.full.html#related-urls**
Email alerting service	Receive free email alerts when new articles cite this article - sign up in the box at the top right corner of the article or **click here**

Unphosphorylated STAT3 accumulates in response to IL-6 and activates transcription by binding to NFκB

Jinbo Yang,[1] Xudong Liao,[1] Mukesh K. Agarwal,[1] Laura Barnes,[1] Philip E. Auron,[2] and George R. Stark[1,3]

[1]Department of Molecular Genetics, Lerner Research Institute, The Cleveland Clinic Foundation, Cleveland, Ohio 44195, USA; [2]Department of Molecular Genetics and Biochemistry, University of Pittsburgh, School of Medicine, Pittsburgh, Pennsylvania 15213, USA

gp130-linked cytokines such as interleukin-6 (IL-6) stimulate the formation of tyrosine-phosphorylated signal transducer and activator of transcription 3 (P-STAT3), which activates many genes, including the STAT3 gene itself. The resulting increase in the concentration of unphosphorylated STAT3 (U-STAT3) drives a second wave of expression of genes such as *RANTES*, *IL6*, *IL8*, *MET*, and *MRAS* that do not respond directly to P-STAT3. Thus, U-STAT3 sustains cytokine-dependent signaling at late times through a mechanism completely distinct from that used by P-STAT3. Many U-STAT3-responsive genes have κB elements that are activated by a novel transcription factor complex formed when U-STAT3 binds to unphosphorylated NFκB (U-NFκB), in competition with IκB. The U-STAT3/U-NFκB complex accumulates in the nucleus with help from the nuclear localization signal of STAT3, activating a subset of κB-dependent genes. Additional genes respond to U-STAT3 through an NFκB-independent mechanism. The role of signal-dependent increases in U-STAT3 expression in regulating gene expression is likely to be important in physiological responses to gp130-linked cytokines and growth factors that activate STAT3, and in cancers that have constitutively active P-STAT3.

Signal transducer and activator of transcription 3 (STAT3), one of seven STAT family members, is activated in response to interleukin-6 (IL-6) (Akira et al. 1994). Many cytokines use the common gp130 receptor to activate the phosphorylation of STAT3 on tyrosine residue 705, leading to the formation of dimers through reciprocal phosphotyrosine–SH2 domain interactions. Several growth factors also stimulate STAT3 activation. STAT3 dimers bind to specific γ-interferon activation sequence (GAS) elements (TTCNNNGAA) in the promoters of the induced genes (Seidel et al. 1995).

Constitutive activation of STAT3 is observed in many types of tumors. Thus, STAT3 is an oncogene, promoting cell proliferation and survival (Haura et al. 2005; Hodge et al. 2005). STAT3 is persistently phosphorylated in many human cancer cell lines and primary tumors, including hepatocellular carcinomas, breast cancers, prostate cancers, and head and neck cancers, and also in several hematological malignances. Furthermore,

STAT3 is necessary for v-src-induced transformation, and a constitutively active mutant of STAT3 can transform fibroblasts in cooperation with other transcription factors (Joo et al. 2004). Genes encoding proteins that regulate cell survival, including Bcl-2, Bcl-xL, mcl-1, and Fas, are direct targets of STAT3, as are genes encoding the cell cycle regulatory proteins cyclin D1, cyclin E1, and p21. In addition, other transcription factors, including c-Myc, c-Jun, and c-Fos, are themselves STAT3 targets (Hirano et al. 2000). STAT3 also functions as a transcriptional repressor of p53 expression: Blocking STAT3 in cancer cells up-regulates the expression of p53, leading to p53-mediated apoptosis (Niu et al. 2005). Major mechanisms of STAT3 activation in tumor cells are autocrine production of IL-6 and paracrine activation by IL-6 from stroma and infiltrating inflammatory cells. Indeed, circulating IL-6 levels are usually high in cancer patients (Giannitrapani et al. 2002). STAT3 activation provides an important link between inflammation and cancer. For example, Tebbutt et al. (2002) generated gp130[757F/F] mice, which carry a Y757F point mutation that disrupts the binding of the negative regulators SOCS3 and SHP2 to gp130. As a result, these mice show

hyperactivation of STAT3, resulting in chronic gastric inflammation and distal stomach tumors.

There are several reports that STAT3 and NF-κB interact with each other (Battle and Frank 2002). For example, Hagihara et al. (2005) demonstrated that STAT3 forms a complex with the p65 subunit of NFκB following stimulation of cells with IL-1 plus IL-6, and that the bound STAT3 interacts with nonconsensus sequences near the κB element of the *SAA* promoter. Moreover, they showed that a complex that includes STAT3, p65, and p300 is essential for the synergistic induction of the *SAA* gene by IL-1 plus IL-6. Yu et al. (2002) reported a physical and functional interaction between STAT3 and p65 that inhibits transcriptional activation of the *iNOS* gene. Yoshida et al. (2004) showed that STAT3 and p65 physically interact in vivo and that p65 homodimers can cooperate with unphosphorylated STAT3 (U-STAT3) when bound to a specific type of κB motif. Reciprocally, this interaction appears to inhibit the function of GAS-binding sites for STAT3. In contrast, the p50 subunit of NFκB can cooperate with phosphorylated STAT3 (P-STAT3) bound to GAS sites (Yoshida et al. 2004).

Previous work from this laboratory has shown that STAT1 can drive gene expression even in the absence of tyrosine phosphorylation. For example, Chatterjee-Kishore et al. (2000) showed that unphosphorylated STAT1 binds to IRF1, forming a complex that activates a half GAS-half ICS element in the *LMP2* promoter. In the case of STAT3, our recent work (Yang et al. 2005) showed that its high-level expression drives the transcription of many genes in the complete absence of tyrosine phosphorylation, a function quite distinct from the role of P-STAT3 in driving inducible gene expression. This activity of STAT3 is likely to have important physiological functions, since the STAT3 gene has a GAS element that drives a major increase in the concentration of STAT3 protein in response to signal-dependent tyrosine phosphorylation of STAT3 (Kojima et al. 1996; Narimatsu et al. 2001). We now address the mechanism through which U-STAT3 regulates gene expression, showing that, for many genes, it does so through its ability to interact with NFκB. To understand how U-STAT3 functions, we expressed the Y705F mutant of STAT3, which cannot be phosphorylated on residue 705, at a high level in untransformed human mammary epithelial hTERT-HME1 cells and used coimmunoprecipitation and chromatin immunoprecipitation (ChIP) assays to identify cofactors and DNA elements to which Y705F-STAT3 binds. Our data reveal that Y705F-STAT3 forms a complex with unphosphorylated NFκB (U-NFκB), binding to the κB elements of promoters, such as that of the *RANTES* (*CCL5*) gene, to induce their transcription.

Results

Promoters that bind to U-STAT3

To find the direct targets of U-STAT3, we used ChIP to clone the bound DNA sequences. Flag-tagged Y705F-STAT3 was precipitated with anti-Flag (M2) antibody.

The coprecipitated DNA fragments were linked to adaptors, amplified by PCR, and inserted into a vector, followed by sequencing of individual clones. A BLAST search facilitated the identification of 12 fragments, seven of which (Table 1) had promoter activity in a luciferase reporter assay (data not shown). Five of the seven active promoter fragments corresponded to genes shown previously to be up-regulated by U-STAT3 (Yang et al. 2005). Computer-based analysis revealed several common elements that bind to transcription factors in these promoters (Ap1, CRE, C/EBP, ETS, and κB) (see Table 1). Interestingly, each of the seven promoters has a κB element.

USTAT3 uses the κB element to induce RANTES gene expression

From previous work (Yang et al. 2005), we know that high-level expression of either U-STAT3 or Y705F-STAT3 drives the expression of many genes, including genes whose protein products are important in oncogenesis, cell cycle control, and the immune response (e.g., *MET*, *MRAS*, *BCL2A1*, *IFN*β, and *RANTES*). Some of these genes are induced very substantially; i.e., *RANTES* was induced 28-fold by high levels of U-STAT3 and 42-fold by Y705F-STAT3. Since *RANTES* expression is induced so strongly, we studied its promoter to determine the role of the κB element. hTERT-HME1 cells were infected with retroviral vectors expressing wild-type or

Table 1. *Promoters that bind to USTAT3 have κB sites*

Gene	Fold induction	Elements
RANTES	42	κβ (–581, –45), CRE, ISRE, Sp1, c-myb, C/EBP-α
IL-8	14	κβ (–571), ETS, c-Jun, C/EBP-α, Smad1/4
IFN-β	14	κβ (–106), ETS, IRF-1, C/EBP-α, Smad1/4
IL-6	6	κβ (–110), ETS, CRE, Smad1/4
ICAM-1	6	κβ (–160), CRE, C/EBP-α, AP-1
Novel gene (KIAA1026) at a CpG island	N/A	κβ (–170), AP-1, C/EBP-α, Smad1/4
Unknown gene	N/A	κβ (–282), CRE, C/EBP-α, AP-1, Smad1/4

A ChIP assay was performed with chromatin from YF cells (containing the Y705F mutant of STAT3) by using anti-Flag M2. The immunoprecipitated DNA was amplified by PCR and cloned, and 12 clones were sequenced. Five of the cloned fragments had no promoter activity in a luciferase reporter assay (data not shown). The seven fragments that did have promoter activity are shown. Five of these were from genes previously shown to be responsive to Y705F-STAT3 and U-STAT3 and two were not analyzed previously (N/A). The fold induction of each of these five genes in response to high-level expression of Y705F-STAT3 is shown, as are the positions of the κB elements and consensus sites for other transcription factors.

Yang et al.

Y705F-STAT3, Flag-tagged at their C termini, and populations expressing 10- to 20-fold more STAT3 than wild-type cells were selected (Fig. 1A). These populations are named WT or YF, respectively. Note that this degree of increase corresponds well to the increase of STAT3 seen 36 h after exposure of hTERT-HME1 cells to IL-6, and, as seen before, *RANTES* mRNA accumulated substantially in response to high-level expression of either U-STAT3 or Y705F-STAT3 (Fig. 1A). To determine the responsible element in the *RANTES* promoter, we transfected hTERT-HME1 cells with constructs containing various fragments of this promoter fused to a luciferase reporter gene. Maximum transcriptional activity was observed

with a –120 to –1 minimal fragment, and removal of this sequence from a longer fragment completely eliminated basal transcription (Fig. 1B). The activity induced in response to high-level expression of Y705F-STAT3 disappeared when the –120 to –1 region of the promoter was deleted (Fig. 1C). Sequence analysis showed that the human *RANTES* promoter contains several known elements; for example, CRE, ISRE, and κB. To test these for function, mutations were introduced into the –220 to –1 region, and the resulting fragments were linked to the pGL2-basic vector and tested in transient transfections of hTERT-HME1 and YF cells (Fig. 1D). Disruption of either the CRE or the ISRE element did not affect the
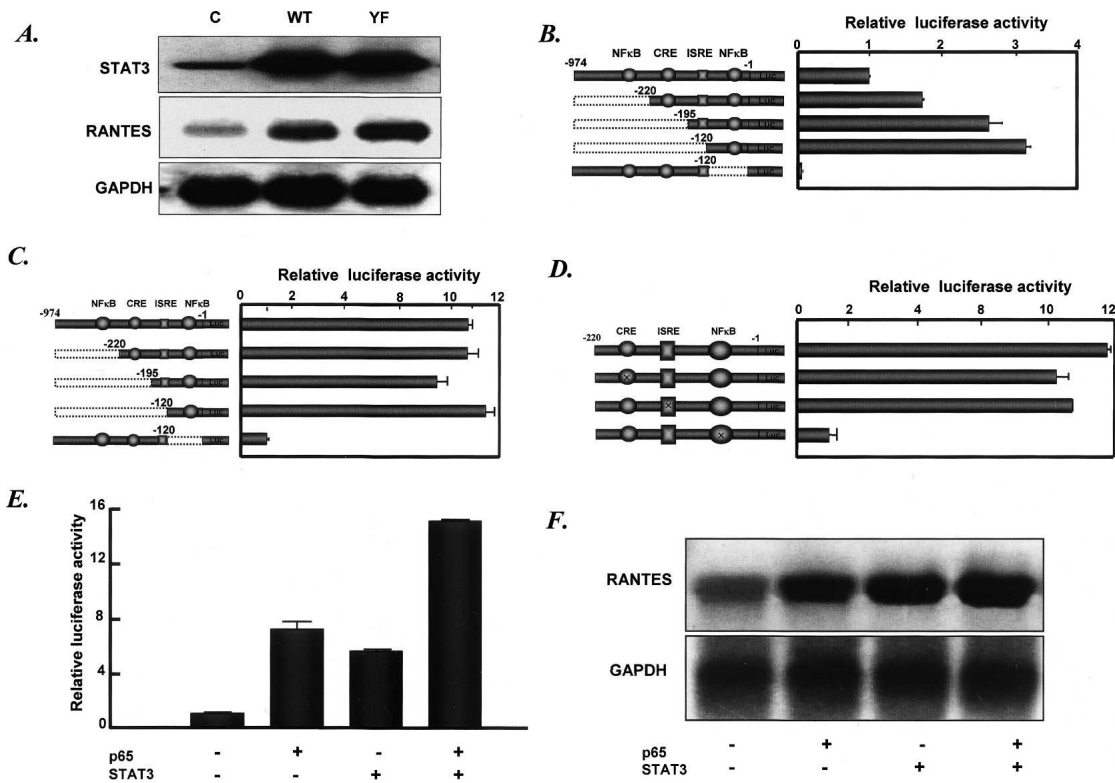
Figure 1. The ability of U-STAT3 to regulate the *RANTES* promoter depends on a κB element. (*A*) Western and Northern analyses for STAT3 and RANTES expression in hTERT-HME1-derived cells. The cells were infected with retroviral constructs and stable pools were selected with G418. (C) hTERT-HME1 control cells; (WT) hTERT-HME1 cells expressing a high level of wild-type STAT3; (YF) hTERT-HME1 cells expressing a high level of Y705F-STAT3. Total cell lysates and total RNAs were analyzed. (*B*) Basal transcriptional activity of the human *RANTES* promoter in hTERT-HME1 cells. Luciferase constructs containing 5′- or 3′-deletions between bases –974 and –1 of the promoter were cotransfected with the pCH110 control plasmid and the cells were harvested 48 h later. The luciferase activity in each cell extract was normalized to the level of β-galactosidase activity (from pCH110) in the same extract. Values are means of triplicate determinations, and the bars show one standard error of the mean. (*C*) Inducible activity of human RANTES promoter fragments in YF cells. The reporter constructs were cotransfected with pCH110. The activities shown are relative to the activity of each fragment in hTERT-HME1 control cells. Values are means of triplicate determinations, and the bars show one standard error of the mean. (*D*) Inducible activity of promoter mutations in YF cells. The reporter constructs, containing mutations of individual promoter elements (marked by ×) of the 220-base-pair promoter fragment were transfected into the cells. Luciferase activities were determined and calculated relative to the values obtained in control cells as in *C*. (*E*) Y705F-STAT3 and p65 cooperate to drive the *RANTES* promoter. hTERT-HME1 cells were cotransfected with the pGL2-220 plasmid, in which the *RANTES* –1 to –220 promoter fragment drives luciferase expression, and pCH110, with or without pcDNA3.1-Y705F-STAT3 or pcDNA3.1-p65, expression plasmids for Y705F-STAT3 and p65, respectively. The cells, harvested 48 h later, were analyzed for luciferase activities, as described above. The reporter activities were normalized to activities in cells without cotransfection of p65 or Y705F-STAT3. Values are means of triplicate determinations, and the bars show one standard error of the mean. (*F*) U-STAT3 and p65 cooperate to activate the *RANTES* gene. hTERT-HME1 cells were transfected transiently with pcDNA3.1-p65 and/or pcDNA3.1-STAT3. After 48 h, total RNAs were isolated and analyzed by the Northern method.

activity of the promoter, but mutation of the κB element did. Therefore, the latter element plays an important role in mediating the response of *RANTES* to U-STAT3.

RANTES *expression is induced cooperatively by p65 and U-STAT3*

Transient overexpression of either the p65 subunit of NFκB or U-STAT3 enhanced induction of the *RANTES* promoter by six- to sevenfold, whereas overexpression of both together led to a 15-fold increase (Fig. 1E). The accumulation of endogenous *RANTES* mRNA was also induced maximally when both p65 and STAT3 were overexpressed (Fig. 1F). Two-step ChIP assays, performed by using anti-STAT3 first and then anti-p65, confirmed that both proteins were bound simultaneously to the *RANTES* promoter (Supplementary Fig. 1). Further experiments showed that overexpression of either U-STAT3 or Y705F-STAT3 did not cause phosphorylation of Ser536 of p65 (Supplementary Fig. 2) and that conditioned medium from these cell populations did not activate expression of either *RANTES* or *IL1β* mRNA (Supplementary Fig. 3). Therefore, the increase in *RANTES* expression in response to U-STAT3 is not likely to be due to the phosphorylation of NFκB in the cytosol or to the secretion of factors that activate NFκB through cell-surface receptors.

A complex of U-STAT3 with the p65 and p50 subunits of NFκB binds to the κB element of the RANTES promoter

Electrophoretic mobility shift assays (EMSAs) were performed with an oligonucleotide that includes the complex κB element of the human *RANTES* promoter. Whole-cell lysates were prepared from hTERT-HME1, wild-type, and YF cells. Two major bands were detected (Fig. 2A, lanes 1–3). We interpret the upper band to include two species, one with p65 homodimers and one with p65–p50 heterodimers, and the lower band to represent species with p50 homodimers. In both wild-type and YF cells, all three bands increased (Fig. 2A, lanes 2,3). Only the upper two bands were supershifted by anti-p65 (Fig. 2A, lane 4), whereas anti-p50 supershifted both the lower band, which disappeared completely, and the lower part of the upper band (Fig. 2A, lane 5). Anti-STAT3 supershifted all three bands (Fig. 2A, lane 6), indicating that all three species of NFκB are bound to Y705F-STAT3. Neither anti-IκB nor anti-c-myc caused any of the bands to change (Fig. 2A, lanes 7,8). When the same cells were treated with TNF-α, EMSAs (Fig. 2A, lanes 9–16) showed that all of the complexes formed in cell extracts containing activated NFκB migrated more rapidly than those formed in extracts of untreated cells. Furthermore, the complexes formed with extracts of TNF-α-treated cells were no longer supershifted by anti-
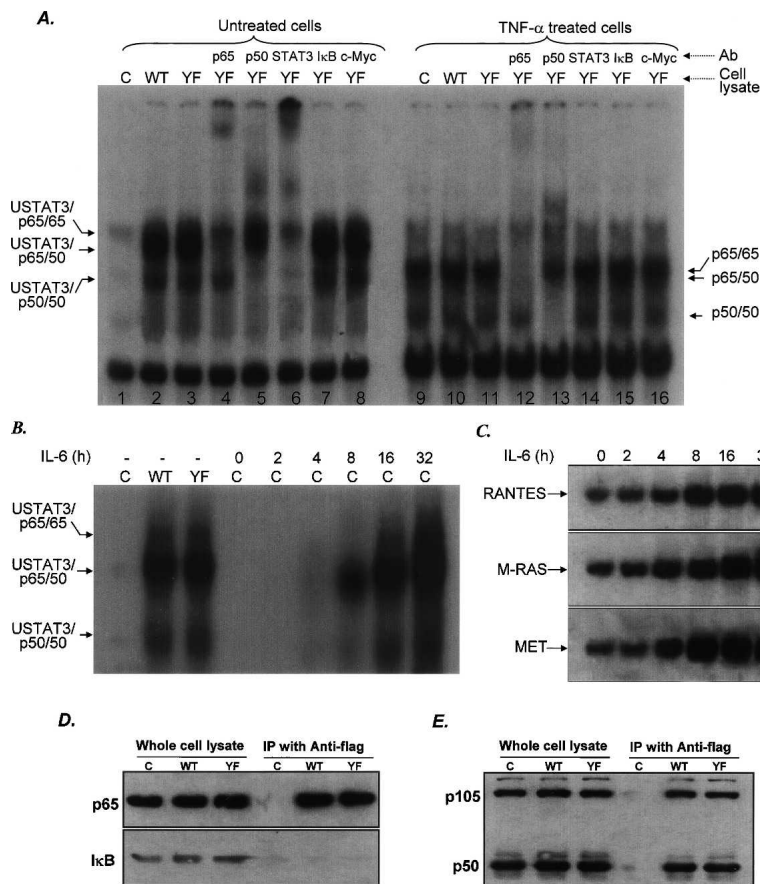
Figure 2. U-STAT3 binds to U-NFκB. (*A*) DNA-binding assays. The EMSAs shown were performed with whole-cell extracts. Assays with nuclear extracts (not shown) gave similar results. (*C*) hTERT-HME1 control cells. A DNA fragment of the human *RANTES* promoter, bases –58 to –29, containing a κB element, was used as the labeled probe. (Lanes *1–8*) Extracts of untreated cells: control cells (lane *1*), WT cells (lane *2*), YF cells (lane *3*), and supershifts obtained with extracts of YF cells following addition of antibodies directed against p65, p50, STAT3, IκB, or c-Myc (lanes *4–8*). (Lanes *9–16*) Same as lanes *1–8* except that the extracts are from cells treated with TNF-α for 4 h. (*B*) EMSAs. Whole-cell extracts were made from hTERT-HME1 cells, untreated or treated with IL-6. The probe was same as in *A*. (*C*) Northern analysis. Total RNAs (20 μg per lane) from hTERT-HME1 cells untreated or treated with IL-6 were analyzed by the Northern method. (*D,E*) STAT3 binds to p65, p50, and p105 but not to IκB. STAT3 was immunoprecipitated from whole-cell extracts of the cells shown in Figure 1A by using anti-Flag M2 beads. Western analyses were performed to detect p65, p50, and IκB.

STAT3 (Fig. 2A, lane 14). Therefore, when cells are treated with TNF-α to activate NFκB, our EMSAs no longer revealed the binding of U-STAT3 to the RANTES κB element together with p65 and p50. However, as shown below, coimmunoprecipitation experiments still detected the association of NFκB and STAT3 when either transcription factor was phosphorylated.

From our previous work (Yang et al. 2005), we know that long-term treatment of hTERT-HME1 cells with IL-6 increases endogenous STAT3 expression by 20- to 30-fold and that the increased concentration of STAT3 induces a second wave of gene expression that includes the *MET*, *M-RAS*, and *RANTES* genes. To determine whether the increased concentration of STAT3 can still bind to and cooperate with p65 and p50 to induce gene expression, hTERT-HME1 cells were treated with IL-6 for 0, 2, 4, 8, 16, or 32 h and EMSAs were performed. As shown in Figure 2B, when STAT3 was induced strongly by IL-6 (Yang et al. 2005; data not shown) at late times, STAT3/p65/p50 complexes were detected in EMSAs. Furthermore, the level of *RANTES* mRNA parallels the level of STAT3 induced by IL-6 (Fig. 2C; Yang et al. 2005), indicating that induced endogenous STAT3, as well as exogenous STAT3 expressed at a high level, is capable of binding to NF-κB to drive gene expression.

U-STAT3 binds to NFκB in competition with IκB

To demonstrate the interaction between NFκB and U-STAT3 more directly, we performed coimmunoprecipitation assays, using wild-type and YF cells, which contain Flag-tagged STAT3 proteins (Fig. 1A). Anti-Flag beads were incubated with lysates of these cells to pull down U-STAT3 and Y705F-STAT3, and the presence of p65 and p50 was assayed in the immunoprecipitates (Fig. 2D,E). P65 and p50, as well as the p50 precursor p105, were pulled down with STAT3, but IκB was not. The levels of p65 and p50 were not affected by the level of STAT3 expression. In addition to its association with unphosphorylated p65, U-STAT3 can also bind to p65 that has been phosphorylated on Ser536 in response to TNF-α (Supplementary Fig. 2). In the EMSA assays of Figure 2A, an association between U-STAT3 or Y705F-STAT3 and NFκB activated in response to TNF-α was not observed, in contrast to the results of Supplementary Figure 2, possibly because complexes of STAT3 and P-NFκB do not bind well to DNA under the EMSA conditions that we have employed. In addition, in cells treated with IL-6, P-STAT3 can also be seen to bind to p65 and p50 (Supplementary Fig. 4; see also Fig. 3 in Yoshida et al. 2004). Therefore, in addition to the association of U-STAT3 and unphosphorylated p65, immunoprecipitation assays reveal that STAT3 and p65 also bind to each other when each is phosphorylated in response to IL-6 or TNF-α, respectively. Furthermore, pulldown experiments using extracts from untreated or IL-6-treated Hep3B cells indicate that both U-STAT3 and P-STAT3 interact primarily with the Rel-homology DNA-binding domain of p65 (Supplementary Fig. 5). The interaction appears to be stronger with the isolated Rel

domain than with full-length p65, suggesting that opening of the interaction between the p65 transactivation domain and the Rel domain may facilitate binding. A similar phenomenon has been reported previously for the interaction between p65 and CBP (Zhong et al. 1998). In addition, as discussed below, several other laboratories have observed interactions between phosphorylated and unphosphorylated forms of p65 and STAT3.
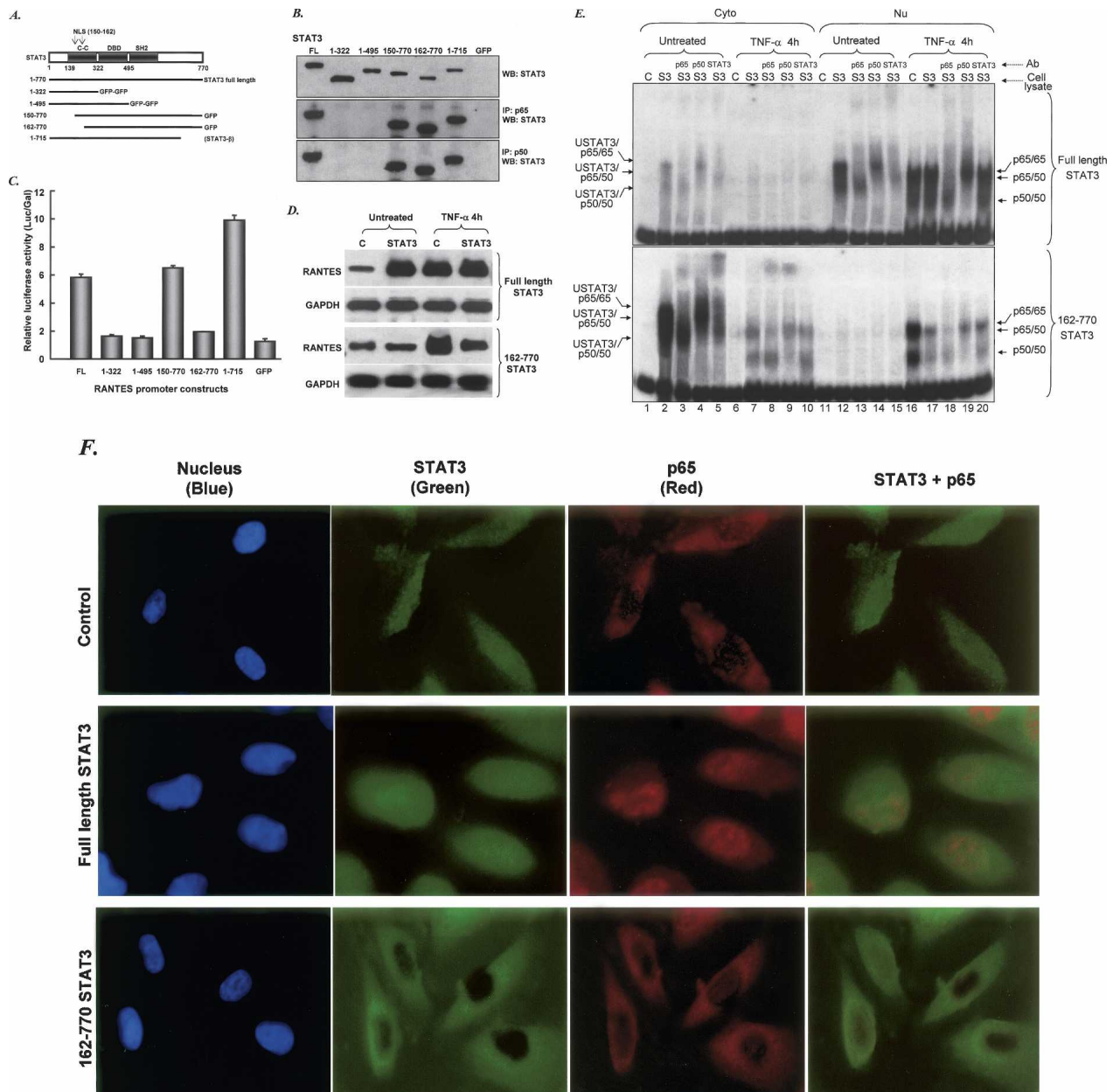
The SH2 and NLS domains of U-STAT3 are required for productive interaction with p65 and p50

We transfected expression constructs for several different truncated GFP-tagged STAT3 proteins (Fig. 3A) transiently into PC3 cells, which have a very low level of endogenous STAT3 (Yuan et al. 2005). Full-length STAT3 (residues 1–770) was immunoprecipitated by both anti-p65 and anti-p50, as were two N-terminal truncations (150–770 and 162–770) and STAT3β (1–715), a naturally occurring C-terminal truncation of this protein. Variant STAT3 proteins with the C-terminal truncations 1–322 and 1–495 did not bind to p65 or p50 (Fig. 3B). These data indicate that the region of STAT3 from 495 to 715, which includes the SH2 domain, is essential for its interaction with NFκB. Functional analysis of these STAT3 deletions, using a *RANTES* promoter-driven luciferase construct in cotransfection experiments, showed that only full-length STAT3 and the 150–770 and 1–715 (STAT3β) truncated proteins were active (Fig. 3C), even though the 162–770 truncated protein still binds to NFκB (Fig. 3B). The 150–770 protein has a nuclear localization sequence (NLS) that the 162–770 protein lacks (Liu et al. 2005). Taken together, the results provide strong evidence that the region between residues 495 and 715, which includes the SH2 domain, is required for U-STAT3 to bind to U-NFκB, whereas the NLS (residues 150–162) is required for the bound protein to function in transcription.

Based on the above observations, it is logical to propose that 162–770 truncated STAT3 may inhibit NFκB-dependent signaling, for example, in response to TNF-α. To test this possibility, hTERT-HME1 cells in which full-length or 162–770 truncated STAT3 was stably overexpressed by 10-fold were treated with TNF-α for 4 h or were untreated. Northern analyses were performed to detect *RANTES* and *GAPDH* mRNAs. As we saw before, high-level expression of full-length STAT3 increases *RANTES* expression by 10- to 20-fold. TNF-α treatment also increases *RANTES* expression by 10- to 15-fold because the *RANTES* gene has a κB element that mediates the response to TNF-α. However, in cells expressing a high level of 162–770 truncated STAT3, untreated cells showed no increases of *RANTES* mRNA and the level in cells treated with TNF-α increased only slightly, by two- to threefold, much less than in control cells treated with TNF-α or in untreated cells expressing a high level of full-length STAT3 (Fig. 3D). This result indicates that 162–770 truncated STAT3 can inhibit NFκB-dependent signaling in response to an external stimulus.

We also performed EMSAs to determine whether trun-

Figure 3. The SH2 and NLS domains of STAT3 are required for interaction with p65 and p50 and for up-regulation of the RANTES promoter. (*A*) STAT3 domains and deletion constructs. (*B*) PC3 cells were transfected with expression constructs for N- and C-terminal deletions of STAT3 and, 48 h later, whole-cell lysates were prepared and assayed by coimmunoprecipitation with anti-p65 or anti-p50 and by the Western method with anti-STAT3. Three different antibodies that react with the N-terminal, C-terminal, and middle portions of STAT3 were used. (*C*) Expression constructs for N- and C-terminal deletions of STAT3 were cotransfected into PC3 cells with pGL2-220 and pCH110, and the cells were harvested for luciferase assays 48 h later. (*D*) Northern analysis. Total RNAs (20 μg per lane) from hTERT-HME1 cells untreated or treated with IL-6 were analyzed by the Northern method. (*E*) DNA-binding assays. hTERT-HME1 cells expressing a high level of full-length STAT3 or 162–770 truncated STAT3 were untreated or treated with TNF-α for 4 h. EMSAs were performed with cytoplasmic and nuclear fractions. A DNA fragment of the human *RANTES* promoter, bases –58 to –29, containing a κB element, was used as the labeled probe. Assays were performed by adding equal amounts of proteins. (C) hTERT-HME1 control cells; (S3) hTERT-HME1 cells expressing a high level of STAT3. (*F*) hTERT-HME1 cells expressing a high level of full-length or 162–770 truncated STAT3 were grown on cover slips and stained with primary antibodies directed against STAT3 and p65. Following treatment with DAPI (blue nuclear stain) and fluorescent secondary antibodies for STAT3 (green) and p65 (red), the cells were examined by using confocal microscopy. The yellow pixels in the composite image demonstrate the close association of the two proteins.

Yang et al.

cated STAT3 affects the ability of the STAT3/p65/p50 complex to bind to a κB probe. hTERT-HME1 cells in which full-length or 162–770 truncated STAT3 was stably expressed at a high level were treated with TNF-α or left untreated. Four hours after treatment, the cells were harvested and cytoplasmic and nuclear fractions were prepared. As expected, full-length STAT3 increased NFκB-binding activity, and the activated complexes were translocated into the nucleus (Fig. 3E, top panel, lanes 1–5,11–15). These increased complexes could be supershifted by antibodies to p65, p50, or STAT3 (Fig. 3E, top panel, lanes 3–5,13–15). TNF-α treatment activates NFκB, and the complexes are located mainly in nucleus (Fig. 3E, top panel, lanes 6–10,16–20). However, these complexes could be supershifted only by antibodies to p65 or p50, but not by anti-STAT3 (Fig. 3E, top panel, lanes 8–10,18–20). 162–770 truncated STAT3 increases NFκB-binding activity only in the cytoplasm and not in the nucleus (Fig. 3E, bottom panel, lanes 1–5,11–15). These cytoplasmic complexes could be supershifted by antibodies to p65, p50, or STAT3 (Fig. 3E, bottom panel, lanes 3–5,13–15). TNF-α treatment is still capable of activating NFκB in these cells, but less than in cells expressing a high level of full-length STAT3 (Fig. 3E, top and bottom panels, lanes 16–20). In TNF-α-treated cells, activated NFκB was translocated into the nucleus completely (Fig. 3E, top and bottom panels, lanes 6,16) indi-

cating that, although 162–770 truncated STAT3 still binds to NFκB, it fails to activate gene expression through a κB element. This observation is consistent with the data from the coimmunoprecipitation and luciferase assays (Fig. 3A–D).

We used immunocytochemistry to demonstrate that STAT3 binds to p65 and p50 in vivo. Full-length or 162–770 truncated STAT3 were expressed at a level fivefold to 10-fold higher than endogenous STAT3, which was detected with a secondary antibody tagged with a green label. Endogenous p65 was detected with a secondary antibody tagged with a red label. In control cells, STAT3 was distributed evenly between the cytoplasm and nucleus, while p65 was seen mainly in the cytoplasm (Fig. 3F, top panel). In cells with a high level of wild-type STAT3, the protein was distributed evenly between the cytoplasm and nucleus as before, but p65 was now seen predominantly in the nucleus (Fig. 3F, middle panel). Interestingly, in cells expressing a high level of 162–770 truncated STAT3, this protein was predominately in the cytoplasm, consistent with the results of others (Liu et al. 2005). As expected, p65 was seen primarily in the cytoplasm, as well (Fig. 3F, bottom panel). By double immunofluorescence we find that the two wild-type proteins are present simultaneously in the nucleus (Fig. 3F, middle panel), consistent with the possibility that STAT3 and p65 indeed do bind to each other in vivo.
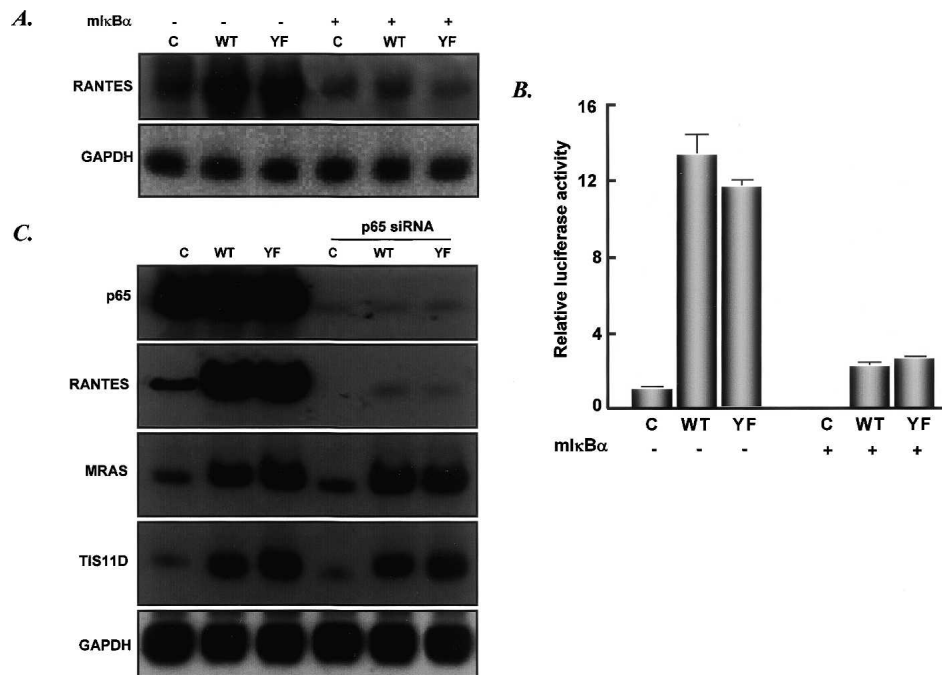
Figure 4. Inhibition of NFκB decreases *RANTES* gene expression in response to U-STAT3. (*A*) hTERT-HME1-derived cells were transfected transiently with the pcDNA3.1-mIκBα construct, which encodes the NFκB superrepressor and, 48 h later, total RNAs were isolated and analyzed. (*B*) The *RANTES* promoter-driven luciferase reporter construct pGL2-220 was transfected with pCH110, with or without pcDNA3.1-mIκBα, into hTERT-HME1-derived cells and, 48 h later, luciferase assays were performed. (*C*) hTERT-HME1-derived cells were transfected transiently with a siRNA directed against p65 and, 24 h later, the cells were transfected again as in *A*. The cells were harvested after 48 h more and total RNA was extracted. All of the mRNAs shown were assayed on the same Northern transfer.

Expression of IκBα superrepressor or ablation of p65 blocks RANTES *expression in response to U-STAT3*

In the absence of an activating signal, the steady-state equilibrium for NFκB localization is toward the cytosol, as a result of interaction with IκB (Birbach et al. 2002). Activating stimuli, such as the proinflammatory cytokines TNF-α and IL-1, liberate NFκB by inducing the phosphorylation of IκB, triggering its ubiquitination and degradation (Henkel et al. 1993; Palombella et al. 1994; Roff et al. 1996). Activation of IκB kinase leads to the phosphorylation of IκBα on Ser32 and Ser36, followed by its rapid proteasome-mediated degradation, allowing free NFκB to enter the nucleus. We were unable to overexpress exogenous wild-type IκB from a construct in these cells (data not shown), probably because it is too unstable when not complexed to p65 and p50. Therefore, we used the serine-to-alanine double mutant of IκBα, S32/36A (mIκBα), which is a superrepressor since it cannot be phosphorylated in response to activating signals. mIκBα was expressed transiently in hTERT-HME1-derived cells, at a level fivefold to 10-fold higher than that of IκB in control cells (data not shown), and mRNA expression from the endogenous *RANTES* gene (Fig. 4A) and *RANTES*-driven promoter (Fig. 4B) were analyzed. As expected, high-level expression of either U-STAT3 or Y705F-STAT3 induced the expression of endogenous *RANTES* mRNA strongly. The inductions were strongly suppressed by mIκBα (Fig. 4A). Similar results were obtained in the luciferase reporter assays (Fig. 4B). To assess the role of p65 in a functional assay, we used an small interfering RNA (siRNA) to cause an almost complete elimination of its expression in all three cell lines (Fig. 4C). The knock down of p65 eliminates both U-STAT3-induced and basal *RANTES* expression. These results provide strong support for a model in which an active transcription complex comprising U-STAT3 and U-NFκB is formed by competition between U-STAT3 and IκB for U-NFκB.

*Array-based expression analysis identifies three subsets of genes responsive to USTAT3 or TNF-α*

The levels of mRNAs isolated from TNF-α-treated or untreated hTERT-HME1-derived cells were analyzed

(Fig. 5A). 1225 genes were induced more than threefold by TNF-α treatment, and 427 genes were induced more than threefold by high-level expression of Y705F-STAT3 (Supplementary Table 1). Of these, 123 genes were induced more than threefold by either TNF-α or by Y705F-STAT3. Therefore, most TNF-α-induced genes are not responsive to a high level of Y705F-STAT3, and most genes induced by Y705F-STAT3 do not respond to TNF-α. Typical genes from each of the three groups were analyzed by the Northern method: *RANTES*, which is induced by both TNF-α and Y705F-STAT3; *IL1β*, which is induced only by TNF-α; and *MAD4*, *MRAS*, and *TIS11D*, which are induced only by Y705F-STAT3 (Fig. 5B). The data clearly show that only a subset of the genes that respond to TNF-α respond also to Y705F-STAT3. Furthermore, many of the genes that respond to Y705F-STAT3 probably do not have functional κB elements, since they do not respond to TNF-α. This possibility was confirmed for MRAS and TIS11D since, in contrast to RANTES, their expression was not affected by eliminating p65 (Fig. 4C).

Discussion

The intracellular concentration of U-STAT3 increases when the STAT3 gene is activated in response to gp130-linked cytokines, allowing U-STAT3 to compete more effectively with IκB for U-NFκB to form a novel transcription factor that induces *RANTES* expression by binding to the proximal κB site of the promoter. Since the Y705F mutant of STAT3, which cannot be phosphorylated on tyrosine, also activates *RANTES* expression, this function of U-STAT3 is clearly distinct from the absolute requirement for tyrosine phosphorylation that enables STAT3 dimers to bind to GAS sequences (Wen et al. 1995; Kaptein et al. 1996; Zhang et al. 1999).

Studies of variant STAT3 proteins in which different domains have been deleted indicate that the region between residues 495 and 715, which includes the SH2 domain, is required for binding to p65 and p50. The small domain between residues 150 and 162 comprises an NLS sequence (Liu et al. 2005) that is necessary to activate gene expression in response to U-STAT3, suggesting that
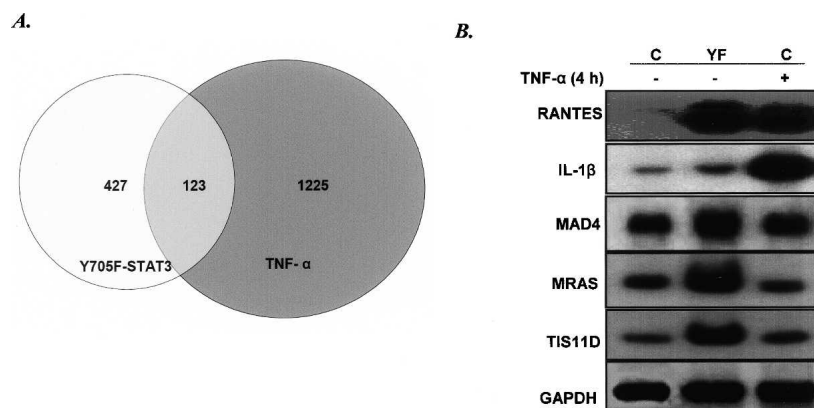
Figure 5. Comparison of genes induced by high-level expression of Y705F-STAT3 with those induced by treatment with TNF-α. hTERT-HME1 control cells or YF cells were treated with 50 ng/mL TNF-α for 4 h or were untreated. Total RNAs were isolated and analyzed by using the CodeLink gene chip system. Genes with a more than threefold change in expression, compared with expression in untreated hTERT-HME1 cells, were scored. (*A*) Comparison of the genes expressed in response to a high level of Y705F-STAT3 or treatment with TNF-α. (*B*) Northern analysis of gene expression.

U-STAT3 contributes to the function of the ternary complex with p65 and p50 by facilitating the nuclear localization of the complex through interaction with importin-α3 (Fig. 6). Additional phosphorylation of P-STAT3 dimers on Ser727 is needed for maximal activation of transcription, but not for DNA binding (Wen and Darnell 1995, 1997). Neither residues 716–770, comprising the transactivation domain of STAT3 (and missing in STAT3β), nor Ser727 are absolutely required for the activity of U-STAT3 on the *RANTES* promoter (Fig. 3). However, it remains possible that the C-terminal domain, together with phosphorylated Ser727, might facilitate the transactivation function of the U-STAT3:U-NFκB complex on other promoters. For example, Ng et al. (2006) have shown that STAT3 is phosphorylated on Ser727 but not Tyr705 in response to activation of the TrkA receptor by nerve growth factor, and that serine-phosphorylated STAT3 is important in driving signal-dependent gene expression. The N-terminal domain of U-STAT3 is not required for binding to NFκB or for function, since the protein that includes residues 150–770 is fully active. Further work is required to delineate in more detail how the individual domains of U-STAT3 function in the ternary complex and to define the relevant domains of p65 and p50. The data of Supplementary Figure 5 already indicate that the Rel domain of p65 is required. Interestingly, the natural increase in the level of U-STAT3 in response to long-term treatment with IL-6 is capable of activating NFκB, and this activation drives the expression of the *RANTES*, *MRAS*, and *MET* genes (Fig. 2B,C). Note that 162–770 truncated STAT3 binds to NFκB but holds the complex in the cytosol, inhibiting the signal-dependent translocation of NFκB into the nucleus and target gene expression (Fig. 3D–F).

Although the binding of U-STAT3 to phosphorylated NFκB is not detected by EMSA under our conditions (Fig. 2A), immunoprecipitation experiments do detect the binding of these two proteins in TNF-α-treated cells

(Supplementary Fig. 2). Conversely, the binding of P-STAT3 to U-NFκB is also detected by immunoprecipitation (Supplementary Figs. 4, 5). Interactions among phosphorylated and unphosphorylated forms of STAT3 and NFκB have been reported previously by several groups. U-STAT3 forms a complex with the p65 subunit of P-NFκB on a κB sequence in the human IL-8 promoter, inducing gene expression in response to IL-1β (Yoshida et al. 2004). U-STAT3 binds to both p65 and p50, and a specific type of κB sequence motif supports both the binding of p65 homodimers and cooperativity with U-STAT3 (Yoshida et al. 2004). Agrawal et al. (2003) showed that P-NFκB synergistically cooperates with P-STAT3 and C/EBPβ to enhance transcription of the C-reactive protein (*CRP*) gene. Hagihara et al. (2005) found that STAT3 plays an essential role in cytokine-driven expression of the serum amyloid A (*SAA*) gene, which does not have a typical STAT3 response element in its promoter. P-STAT3 and P-p65 form a complex following stimulation of cells with both IL-1 and IL-6, after which STAT3 interacts with nonconsensus sequences at the 3′ boundary of κB element of the *SAA* promoter to enhance transcription. Yu et al. (2002) found that U-STAT3, through direct interaction with p65, serves as a dominant-negative inhibitor of the ability of P-NFκB to induce cytokine-dependent induction of the *iNOS* promoter in mesangial cells.

In addition to its interactions with NFκB, STAT3 has been shown to bind to other transcription factors. For example, it forms a complex with the CRE-binding protein on the *JUNB* promoter (Kojima et al. 1996) and with c-Jun on the α2-macrogloblin APRE (Schaefer et al. 1995). Other reports show that STAT3 has an effect on CRE-like sites in the *C/EBPB* promoter (Niehof et al. 2001) and the glucocorticoid response element (Zhang and Fuller 1997; Zhang et al. 1999), which lack classical GAS sequences. We found that fewer than half of the genes that respond to high-level expression of Y705F-

Figure 6. Interactions between the STAT3 and NFκB pathways. U-STAT3, induced to a high level due to activation of the STAT3 gene in response to ligands such as IL-6, competes with IκB for p65/p50. The U-STAT3:U-NFκB complex activates the *RANTES* promoter plus a subset of other promoters that have κB elements. U-STAT3 also drives the expression of some genes that do not have κB elements, by an unknown mechanism (not shown). The κB element of the IL6 gene is driven by canonical NFκB signaling in response to ligands such as TNF-α or IL-1, setting up the positive feedback loop that is driven by the activation of STAT3 in response to secreted IL-6, leading to an increased level of U-STAT3 that sustains the activation of genes such as *RANTES*. (Imp-α3) Importin-α3.
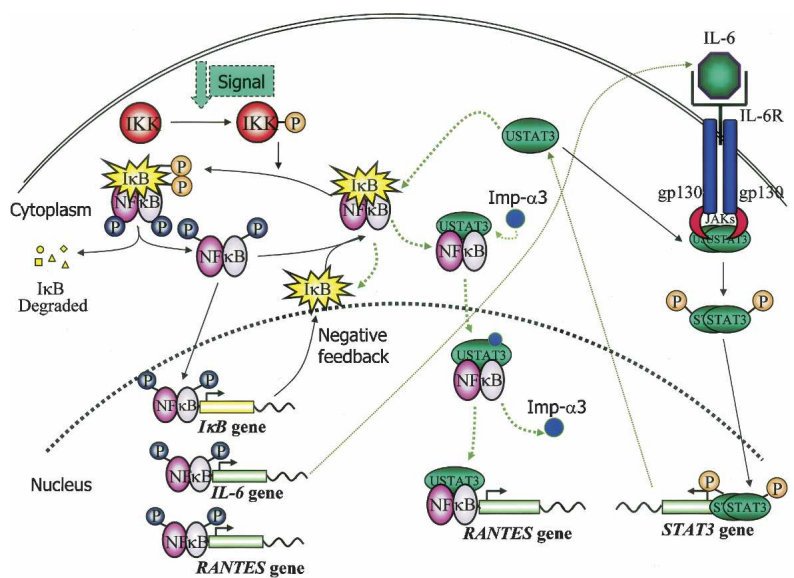
STAT3 respond also to TNF-α (Fig. 5). The Y705F-STAT3-responsive genes that do not respond to TNF-α probably do not have functional κB elements and, as shown in Figure 4C, two such genes do not need p65 in order to respond to Y705F-STAT3. Therefore, it is extremely likely that Y705F-STAT3 (or U-STAT3) interacts productively with one or more transcription factors different from NFκB to drive the expression of this class of genes. Identification of these factors and characterization of their interactions with U-STAT3 remain to be accomplished.

Interconnections between signaling pathways that use activated NFκB and those that use activated STAT3 are shown in Figure 6. The current work reveals the importance of U-STAT3 in connections between these two important classes of pathways. IL-1 is an important mediator of the inflammatory response since it induces other proinflammatory cytokines, chemokines, and acute phase proteins (Dinarello 1996). From the work presented here, we can now appreciate that the expression of IL-6 in response to activation of NFκB by IL-1 initiates a positive feedback loop in which secreted IL-6 stimulates the tyrosine phosphorylation of STAT3, leading secondarily to an increase in U-STAT3, which then drives the expression of a subset of NFκB-activated genes, including *RANTES*. Thus, the κB element of the *RANTES* promoter can function to give strong expression in two ways, directly in response to TNF-α or IL-1 or indirectly in response to IL-6 (Fig. 6). This dual regulation of *RANTES* transcription may be important in regulating its physiological functions, with short-term expression in response to IL-1 controlled by P-NFκB and more sustained expression, indirectly in response to IL-6, regulated by U-STAT3:P-NFκB (Fig. 6).

RANTES is an important mediator of acute and chronic inflammation, with genetic evidence indicating its involvement in immunopathological disorders (Kim et al. 2004; Simeoni et al. 2004; Boger et al. 2005; Wang et al. 2005; Charo and Ransohoff 2006). Its wide spectrum of biological activities is transduced through three distinct chemokine receptors, CCR1, CCR3, and CCR5. These targets of RANTES are present on a diversity of leukocytes, including memory T cells, eosinophils, and monocytes (Fujisawa et al. 2000; Luther and Cyster 2001). Depending on the cellular context, RANTES can deliver chemoattractant or activating signals, with the latter inducing responses of dendritic cells that range from eosinophil degranulation to production of cytokines. The levels of *RANTES* mRNA (Fig. 2C) and the mRNAs encoding *MET*, *MRAS*, and *TIS11D* (Fig. 2C; Yang et al. 2005) are increased coordinately with U-STAT3 levels in cells treated with IL-6 for long times (32–48 h). Sustained RANTES expression, as might be driven by increased expression of U-STAT3 following exposure of cells to gp130-linked cytokines, may be highly significant biologically. For example, elevated RANTES levels can impair the entry into cells of macrophage-tropic HIV-1 via CCR5 (Simmons et al. 2000). Also, micromolar concentration of RANTES can deliver costimulatory signals to T cells, augmenting responses

through the T-cell receptor (Bacon et al. 1995). Elegant structural studies indicate that these concentrations may be achievable in vivo through formation of multimeric RANTES aggregates on a glycosaminoglycan substrate (Johnson et al. 2004; Shaw et al. 2004; Proudfoot 2006). Although the expression of RANTES was first thought to be limited to active T cells, recent data have shown that it is produced by a variety of tissue types in response to specific stimuli. *RANTES* mRNA is expressed late (3–5 d) after activation of resting T cells, whereas in fibroblasts, renal epithelial, and mesangial cells, RANTES mRNA is quickly up-regulated by TNF-α stimulation (Hirano et al. 2003; Ogura et al. 2005).

The full biological relevance of the ability of P-STAT3 to increase the intracellular concentration of U-STAT3 remains to be established. In the context of cancer, the constitutive tyrosine phosphorylation of STAT3 in many different tumors is likely to lead to increased expression of U-STAT3, which in turn drives the expression of oncogenes such as MET and MRAS (Yang et al. 2005). In cell culture system, long-term treatment with IL-6 to increase total U-STAT3, the expression levels for *RANTES*, as well as *MET*, *MRAS*, and *TIS11D* (Fig. 2C; Yang et al. 2005) are increased coordinately with U-STAT3 levels at late IL-6-treated time points (32–48 h). The biological role of U-STAT3-driven gene expression in normal physiology is best addressed by experiments with genetically altered mice. An important attempt to do this was reported by Narimatsu et al. (2001), who mutated the GAS element of the endogenous *STAT3* promoter. The ability of IL-6 to increase STAT3 expression was abrogated in some tissues but not in others, probably because STAT3-dependent expression of the *STAT3* gene can be regulated through additional elements that were not recognized and therefore were not mutated. Incomplete suppression of the response of the *STAT3* gene to IL-6 might well account for the observed mild phenotype of the promoter knock-in mouse. Since complete deletion of *STAT3* is embryonic lethal (Takeda et al. 1997), it remains to be seen whether mice with complete loss of the STAT3-dependent induction of U-STAT3 expression would have severe defects, as might be expected if the up-regulation of U-STAT3 is important for the full physiological functions of the many cytokines that use the common gp130 receptor subunit to phosphorylate STAT3.

Materials and methods

Cells and reagents

hTERT-HME1 cells (Clontech) were grown in MCDB 170 medium with supplements of bovine pituitary extract, hydrocortisone, insulin, gentamycin, human epidermal growth factor, and amphotericin-B, all from Clonetics. PC3 cells were grown in Dulbecco's Modified Eagle's Medium (DMEM) supplemented with 10% fetal bovine serum (FBS) and penicillin (100 U/mL) and streptomycin (100 μg/mL) (GIBCO-BRL). TNF-α was used at a concentration of 50 ng/mL. Antibodies against STAT3 (C-20, K-15, and H-190), p65, p50, IκBα, and c-Myc were from Santa Cruz Biotechnologies, and antibodies against Tyr705-phosphorylated STAT3 (pTyr-STAT3) and Ser536-phosphorylated

p65 were from Cell Signaling Technology. WT and YF cells, expressing a high level of wild-type STAT3 or Y705F-STAT3, respectively, were described previously (Yang et al. 2005). The construct for truncated 162–770 wild-type STAT3 and cells expressing a high level of this protein were generated as described before (Yang et al. 2005). Plasmids encoding GFP-tagged STAT3 N- and C-terminal deletion mutants were generous gifts from Nancy C. Reich, State University of New York, Stony Brook, Stony Brook, NY (Liu et al. 2005). The p65 expression plasmid was described by Yoshida et al. (2004). NFκB siRNA was from Cell Signaling Technology.

Luciferase reporter plasmid

A 1.5-kb DNA fragment containing the human *RANTES* promoter (–1426 to +128), obtained from a ChIP experiment, was inserted to the pcDNA3.1 vector. *RANTES* promoter deletion and mutation reporter constructs were gifts from Dr. Antonella Casola, University of Texas Medical Branch, Galveston, TX (Casola et al. 2002). Further deletions of these luciferase reporter constructs were performed by PCR, by introducing KpnI and NheI sites, followed by subcloning to the same restriction sites of the pGL2-basic vector, to generate pGL2-974 (–974 ~ –1), pGL2-220 (–220 ~ –1), pGL2-195 (–195 ~ –1), pGL2-120 (–120 ~ –1), pGL2-del (–974 ~ –120), pGL2-CRE-m (5'-AAACT GATGAGCTCACTCTA-3' to 5'-AAACTtcTtAtagacCgCTA -3'), pGL2-ISRE-m (5'-TTTCAGTTTTCTTTTCC-3' to 5'-TT TCAGTaaaCTaaaCC-3'), and pGL2-NFκB-m (5'-TTTTGGAAA CTCCCCTTAGGGGATGCCCT-3' to 5'-TTTTGGcAcCTtaa CgTA cGCCATGCatT-3'), respectively (Casola et al. 2002). Note that the *RANTES* promoter sequence used has two κB sites and that both were mutated. To guard against PCR-associated incorporation errors, the integrity of all the constructs generated was confirmed by sequencing.

Transfection and luciferase assays

RANTES promoter–luciferase reporter (Luc) constructs were transfected into hTERT-HME1 cells by using the Fugene 6 reagent (Roche). Cells were plated and cultured in 12-well plates to 40% confluence before transfection. After a change to fresh media, 1 µg/well luciferase plasmid plus 0.5 µg/well pCH110 (β-galactoside plasmid for internal control) were cotransfected. Forty hours later, the cells were harvested and the cell pellets were lysed in 200 µL of buffer (Reporter lysis buffer, Promega), mixed by vortexing for 5 sec, and spun at 2000*g* for 5 min at room temperature. Cell lysate (60 µL) was mixed with 60 µL of luciferase assay buffer (Promega) for activity measurements in an Auto Lumat BG-P luminometer (MGM Instruments). For the β-galactosidase activity assay, the luminescent β-galactosidase detection Kit II (Clontech) was used.

p65 siRNA transfection

hTERT-HME1-derived cells were grown in 60-mm plates to 40% confluence before transfection. Media were aspirated from the cells, which were washed twice with sterile phosphate-buffered saline. Then, 5 mL of fresh medium were added to each plate, with 10% serum and without antibiotics. Twenty microliters of 10 µM p65 siRNA (Cell Signaling Technology) were added to 300 µL of siRNA Transfection Medium (Santa Cruz Biotechnology), mixed gently, kept at room temperature for 20 min, and added drop-wise to the plates with gentle rocking. After incubation for 24 h at 37°C, the transfection media were removed and the cells were transfected again, following the

same protocol. After another 48 h, the cells were harvested and total RNA or protein was extracted for analysis.

Coimmunoprecipitations

The protocol provided by Sigma-Aldrich was followed, with slight modifications. For immunoprecipitation of p65, cells were lysed in buffer (50 mM Tris HCl at pH 8.0, 150 mM NaCl, 1% NP-40) and Sepharose G beads were used. For immunoprecipitation of STAT3, the EZview Red ANTI-FLAG M2 Affinity Gel system (Sigma-Aldrich) was used, exactly as in the protocol provided by the manufacturer.

Western and Northern analyses

These procedures were carried out essentially as described before (Yang et al. 2005). For Western analyses, membranes were probed with primary antibodies specific for STAT3 (Santa Cruz Biotechnology, 482), Tyr705-STAT3, p65 (Santa Cruz Biotechnology, 109), p50 (Santa Cruz Biotechnology, 114), or Ser536-p65. For Northern analyses, 20 µg of total RNA were used. Human cDNA probes for *RANTES*, *MET*, *IL1*β, *MAD4*, *MRAS*, and *TIS11D* were cut from I.M.A.G.E. clones (Invitrogen or the American Type Culture Collection). Templates for the human GAPDH cDNA were obtained by RT–PCR. Signals were normalized for loading by comparing the intensities of GAPDH mRNA on the same membranes.

EMSAs

This procedure was performed as reported previously (Yang et al. 2005). hTERT-HME1-derived cells, untreated or treated with TNF-α for 4 h, were lysed in EMSA lysis buffer, supplemented with protease inhibitors. The probe was the NFκB consensus sequence (top strand, 5'-TTTTGGAAACTCCCCTTAGGGGA TGCCCCT-3') from the *RANTES* promoter (Nelson et al. 1993; Genin et al. 2000). Labeled probe (10^4 DPM) was used in each binding reaction. For supershift analyses, whole-cell extracts were preincubated for 20 min at room temperature with polyclonal antibodies specific for STAT3, p65, p50 (see above), IκB (Santa Cruz Biotechnology, 371), or c-Myc (Santa Cruz Biotechnology, 788) before adding radiolabeled probe.

ChIP analyses

The protocol is from previous publications (Weinmann and Farnham 2002; Li et al. 2003). Briefly, 10^8 cells were cross-linked in 1% formaldehyde for 10 min before adding 0.125 M glycine to terminate the reaction. The cells were trypsinized and resuspended in 6 mL of cell lysis buffer (5 mM PIPES at pH 8.0, 85 mM KCl, 0.5% Nonidet P-40, 10 µL/mL PMSF, 1 µL/mL aprotinin, 1 µL/mL leupeptin). After incubation for 10 min on ice, nuclei were collected and resuspended in 1 mL of nuclear lysis buffer (50 mM Tris HCl at pH 8.1, 10 mM EDTA, 1% SDS) plus protease inhibitors to obtain chromatin preparations, which were then sonicated to an average length of ~0.5–2 kb by using 15 pulses of 30 sec each with 2-min rests at setting 5 of a Fisher Model 60 sonic dismembranator. Sonicated samples were immunoprecipitated with anti-M2 (anti-Flag), which distinguishes exogenous (tagged) from endogenous (untagged) U-STAT3. The cross-links were then reversed in 0.3 M NaCl in the presence of RNaseA (Roche), 10 mg/mL, for 4–5 h at 65°C. DNA fragments were purified by ethanol precipitation. The immunoprecipitated DNA was amplified by a ligation-mediated PCR (LM–PCR) procedure in which the samples were pretreated with T4 DNA polymerase to blunt the ends of the DNA. Then

a linker was ligated to the DNA fragments, allowing them to be amplified by PCR, using primers located in the linker. The PCR products were ligated into a pcDNA3.1-based vector by using Rapid Ligation Kit (Roche). Inserts were sequenced by using a vector-specific primer and T7 or Sp6 polymerase.

CodeLink expression array experiments

Total RNAs were analyzed by using CodeLink arrays (GenUs Biosystems). Data were analyzed by using GenUs software. Expression was normalized against the levels of GAPDH and ACTIN mRNAs in the all samples. The levels of mRNAs in TNF-α-treated cells or untreated YF cells were compared with the levels in hTERT-HME1 control cells. The data are presented in Supplementary Table 1.

Immunocytochemistry

hTERT-HME1 cells stably expressing a high level of full-length wild-type STAT3 or 162–770 truncated STAT3 (Yang et al. 2005) were grown on glass cover slips for 24 h before fixation. Cells at ~50% confluency were fixed in 4% paraformaldehyde for 15 min and absolute methanol for 5 min at room temperature and then treated with blocking buffer (1× PBS + 0.3% Triton X-100 + 10% FBS). STAT3 was detected with mouse anti-human STAT3 (Cell Signaling Technology) and rabbit anti-human p65 (Santa Cruz Biotechnology). Signals were visualized by Alexa Fluor 488 goat anti-mouse (green fluorescent) and Alexa Fluor 494 goat anti-rabbit (red fluorescent) secondary antibodies. Images were captured with a Zeiss Axioskop fluorescence microscope.

Acknowledgments

References

Agrawal, A., Cha-Molstad, H., Samols, D., and Kushner, I. 2003. Overexpressed nuclear factor-κB can participate in endogenous C-reactive protein induction, and enhances the effects of C/EBPβ and signal transducer and activator of transcription-3. *Immunology* **108:** 539–547.

Akira, S., Nishio, Y., Inoue, M., Wang, X.J., Wei, S., Matsusaka, T., Yoshida, K., Sudo, T., Naruto, M., and Kishimoto, T. 1994. Molecular cloning of APRF, a novel IFN-stimulated gene factor 3 p91-related transcription factor involved in the gp130-mediated signaling pathway. *Cell* **77:** 63–71.

Bacon, K.B., Premack, B.A., Gardner, P., and Schall, T.J. 1995. Activation of dual T cell signaling pathways by the chemokine RANTES. *Science* **269:** 1727–1730.

Battle, T.E. and Frank, D.A. 2002. The role of STATs in apoptosis. *Curr. Mol. Med.* **2:** 381–392.

Birbach, A., Gold, P., Binder, B.R., Hofer, E., de Martin, R., and Schmid, J.A. 2002. Signaling molecules of the NF-κB pathway shuttle constitutively between cytoplasm and nucleus. *J. Biol. Chem.* **277:** 10842–10851.

Boger, C.A., Fischereder, M., Deinzer, M., Aslanidis, C., Schmitz, G., Stubanus, M., Banas, B., Kruger, B., Riegger, G.A., and Kramer, B.K. 2005. RANTES gene polymorphisms predict all-cause and cardiac mortality in type 2 diabetes mellitus hemodialysis patients. *Atherosclerosis* **183:** 121–129.

Casola, A., Henderson, A., Liu, T., Garofalo, R.P., and Brasier, A.R. 2002. Regulation of RANTES promoter activation in alveolar epithelial cells after cytokine stimulation. *Am. J. Physiol. Lung Cell. Mol. Physiol.* **283:** L1280–L1290.

Charo, I.F. and Ransohoff, R.M. 2006. The many roles of chemokines and chemokine receptors in inflammation. *N. Engl. J. Med.* **354:** 610–621.

Chatterjee-Kishore, M., Wright, K.L., Ting, J.P., and Stark, G.R. 2000. How Stat1 mediates constitutive gene expression: A complex of unphosphorylated Stat1 and IRF1 supports transcription of the LMP2 gene. *EMBO J.* **19:** 4111–4122.

Dinarello, C.A. 1996. Biologic basis for Interleukin-1 in disease. *Blood* **87:** 2095–2147.

Fujisawa, T., Kato, Y., Nagase, H., Atsuta, J., Terada, A., Iguchi, K., Kamiya, H., Morita, Y., Kitaura, M., Kawasaki, H., et al. 2000. Chemokines induce eosinophil degranulation through CCR-3. *J. Allergy Clin. Immunol.* **106:** 507–513.

Genin, P., Algarte, M., Roof, P., Lin, R., and Hiscott, J. 2000. Regulation of RANTES chemokine gene expression requires cooperativity between NF-κ B and IFN-regulatory factor transcription factors. *J. Immunol.* **164:** 5352–5361.

Giannitrapani, L., Cervello, M., Soresi, M., Notarbartolo, M., La Rosa, M., Virruso, L., D'Alessandro, N., and Montalto, G. 2002. Circulating IL-6 and sIL-6R in patients with hepatocellular carcinoma. *Ann. N. Y. Acad. Sci.* **963:** 46–52.

Hagihara, K., Nishikawa, T., Sugamata, Y., Song, J., Isobe, T., Taga, T., and Yoshizaki, K. 2005. Essential role of STAT3 in cytokine-driven NF-κB-mediated serum amyloid A gene expression. *Genes Cells* **10:** 1051–1063.

Haura, E.B., Turkson, J., and Jove, R. 2005. Mechanisms of disease: Insights into the emerging role of signal transducers and activators of transcription in cancer. *Nat. Clin. Pract. Oncol.* **2:** 315–324.

Henkel, T., Machleidt, T., Alkalay, I., Kronke, M., Ben-Neriah, Y., and Baeuerle, P.A. 1993. Rapid proteolysis of IκBα is necessary for activation of transcription factor NF-κB. *Nature* **365:** 182–185.

Hirano, T., Ishihara, K., and Hibi, M. 2000. Roles of STAT3 in mediating the cell growth, differentiation and survival signals relayed through the IL-6 family of cytokine receptors. *Oncogene* **19:** 2548–2556.

Hirano, F., Komura, K., Fukawa, E., and Makino, I. 2003. Tumor necrosis factor α TNF-α-induced RANTES chemokine expression via activation of NF-κB and p38 MAP kinase: Roles of TNF-α in alcoholic liver diseases. *J. Hepatol.* **38:** 483–489.

Hodge, D.R., Hurt, E.M., and Farrar, W.L. 2005. The role of IL-6 and STAT3 in inflammation and cancer. *Eur. J. Cancer* **41:** 2502–2512.

Johnson, Z., Kosco-Vilbois, M.H., Herren, S., Cirillo, R., Muzio, V., Zaratin, P., Carbonatto, M., Mack, M., Smailbegovic, A., Rose, M., et al. 2004. Interference with heparin binding and oligomerization creates a novel anti-inflammatory strategy targeting the chemokine system. *J. Immunol.* **173:** 5776–5785.

Joo, A., Aburatani, H., Morii, E., Iba, H., and Yoshimura, A. 2004. STAT3 and MITF cooperatively induce cellular transformation through upregulation of c-fos expression. *Onco-*

gene **23:** 726–734.

Kaptein, A., Paillard, V., and Saunders, M. 1996. Dominant negative stat3 mutant inhibits interleukin-6-induced Jak–STAT signal transduction. *J. Biol. Chem.* **271:** 5961–5964.

Kim, J.J., Lee, J.H., Jang, C.H., Kim, Y.S., Chae, S.C., Chung, H.T., Choi, T.W., and Lee, J.H. 2004. Chemokine RANTES promoter polymorphisms in allergic rhinitis. *Laryngoscope* **114:** 666–669.

Kojima, H., Nakajima, K., and Hirano, T. 1996. IL-6-inducible complexes on an IL-6 response element of the junB promoter contain Stat3 and 36 kDa CRE-like site binding proteins. *Oncogene* **12:** 547–554.

Li, Z., Van Calcar, S., Qu, C., Cavenee, W.K., Zhang, M.Q., and Ren, B. 2003. A global transcriptional regulatory role for c-Myc in Burkitt's lymphoma cells. *Proc. Natl. Acad. Sci.* **100:** 8164–8169.

Liu, L., McBride, K.M., and Reich, N.C. 2005. STAT3 nuclear import is independent of tyrosine phosphorylation and mediated by importin-α3. *Proc. Natl. Acad. Sci.* **102:** 8150–8155.

Luther, S.A. and Cyster, J.G. 2001. Chemokines as regulators of T cell differentiation. *Nat. Immunol.* **2:** 102–107.

Narimatsu, M., Maeda, H., Itoh, S., Atsumi, T., Ohtani, T., Nishida, K., Itoh, M., Kamimura, D., Park, S.J., Mizuno, K., et al. 2001. Tissue-specific autoregulation of the stat3 gene and its role in interleukin-6-induced survival signals in T cells. *Mol. Cell. Biol.* **21:** 6615–6625.

Nelson, P.J., Kim, H.T., Manning, W.C., Goralski, T.J., and Krensky, A.M. 1993. Genomic organization and transcriptional regulation of the RANTES chemokine gene. *J. Immunol.* **151:** 2601–2612.

Ng, Y.P., Cheung, Z.H., and Ip, N.Y. 2006. STAT3 as a downstream mediator of Trk signaling and functions. *J. Biol. Chem.* **281:** 15636–15644.

Niehof, M., Streetz, K., Rakemann, T., Bischoff, S.C., Manns, M.P., Horn, F., and Trautwein, C. 2001. Interleukin-6-induced tethering of STAT3 to the LAP/C/EBPβ promoter suggests a new mechanism of transcriptional regulation by STAT3. *J. Biol. Chem.* **276:** 9016–9027.

Niu, G., Wright, K.L., Ma, Y., Wright, G.M., Huang, M., Irby, R., Briggs, J., Karras, J., Cress, W.D., Pardoll, D., et al. 2005. Role of Stat3 in regulating p53 expression and function. *Mol. Cell. Biol.* **25:** 7432–7440.

Ogura, N., Tobe, M., Sakamaki, H., Nagura, H., Abiko, Y., and Kondoh, T. 2005. Tumor necrosis factor-α increases chemokine gene expression and production in synovial fibroblasts from human temporomandibular joint. *J. Oral Pathol. Med.* **34:** 357–363.

Palombella, V.J., Rando, O.J., Goldberg, A.L., and Maniatis, T. 1994. The ubiquitin-proteasome pathway is required for processing the NF-κB precursor protein and the activation of NF-κB. *Cell* **78:** 773–785.

Proudfoot, A.E. 2006. The biological relevance of chemokine–proteoglycan interactions. *Biochem. Soc. Trans.* **34:** 422–426.

Roff, M., Thompson, J., Rodriguez, M.S., Jacque, J.M., Baleux, F., Arenzana-Seisdedos, F., and Hay, R.T. 1996. Role of IκBα ubiquitination in signal-induced activation of NFκB in vivo. *J. Biol. Chem.* **271:** 7844–7850.

Schaefer, T.S., Sanders, L.K., and Nathans, D. 1995. Cooperative transcriptional activity of Jun and Stat3 β, a short form of Stat3. *Proc. Natl. Acad. Sci.* **92:** 9097–9101.

Seidel, H.M., Milocco, L.H., Lamb, P., Darnell Jr., J.E., Stein, R.B., and Rosen, J. 1995. Spacing of palindromic half sites as a determinant of selective STAT signal transducers and activators of transcription DNA binding and transcriptional activity. *Proc. Natl. Acad. Sci.* **92:** 3041–3045.

Shaw, J.P., Johnson, Z., Borlat, F., Zwahlen, C., Kungl, A., Rou-

lin, K., Harrenga, A., Wells, T.N., and Proudfoot, A.E. 2004. The X-ray structure of RANTES: Heparin-derived disaccharides allows the rational design of chemokine inhibitors. *Structure* **12:** 2081–2093.

Simeoni, E., Winkelmann, B.R., Hoffmann, M.M., Fleury, S., Ruiz, J., Kappenberger, L., Marz, W., and Vassalli, G. 2004. Association of RANTES G-403A gene polymorphism with increased risk of coronary arteriosclerosis. *Eur. Heart J.* **25:** 1438–1446.

Simmons, G., Reeves, J.D., Hibbitts, S., Stine, J.T., Gray, P.W., Proudfoot, A.E., and Clapham, P.R. 2000. Co-receptor use by HIV and inhibition of HIV infection by chemokine receptor ligands. *Immunol. Rev.* **177:** 112–126.

Takeda, K., Noguchi, K., Shi, W., Tanaka, T., Matsumoto, M., Yoshida, N., Kishimoto, T., and Akira, S. 1997. Targeted disruption of the mouse Stat3 gene leads to early embryonic lethality. *Proc. Natl. Acad. Sci.* **94:** 3801–3804.

Tebbutt, N.C., Giraud, A.S., Inglese, M., Jenkins, B., Waring, P., Clay, F.J., Malki, S., Alderman, B.M., Grail, D., Hollande, F., et al. 2002. Reciprocal regulation of gastrointestinal homeostasis by SHP2 and STAT-mediated trefoil gene activation in gp130 mutant mice. *Nat. Med.* **8:** 1089–1097.

Wang, C.R., Guo, H.R., and Liu, M.F. 2005. RANTES promoter polymorphism as a genetic risk factor for rheumatoid arthritis in the Chinese. *Clin. Exp. Rheumatol.* **23:** 379–384.

Weinmann, A.S. and Farnham, P.J. 2002. Identification of unknown target genes of human transcription factors using chromatin immunoprecipitation. *Methods* **26:** 37–47.

Wen, Z. and Darnell Jr., J.E. 1997. Mapping of Stat3 serine phosphorylation to a single residue 727 and evidence that serine phosphorylation has no influence on DNA binding of Stat1 and Stat3. *Nucleic Acids Res.* **25:** 2062–2067.

Wen, Z., Zhong, Z., and Darnell Jr., J.E. 1995. Maximal activation of transcription by Stat1 and Stat3 requires both tyrosine and serine phosphorylation. *Cell* **82:** 241–250.

Yang, J., Chatterjee-Kishore, M., Staugaitis, S.M., Nguyen, H., Schlessinger, K., Levy, D.E., and Stark, G.R. 2005. Novel roles of unphosphorylated STAT3 in oncogenesis and transcriptional regulation. *Cancer Res.* **65:** 939–947.

Yoshida, Y., Kumar, A., Koyama, Y., Peng, H., Arman, A., Boch, J.A., and Auron, P.E. 2004. Interleukin 1 activates STAT3/nuclear factor-κB cross-talk via a unique TRAF6- and p65-dependent mechanism. *J. Biol. Chem.* **279:** 1768–1776.

Yu, Z., Zhang, W., and Kone, B.C. 2002. Signal transducers and activators of transcription 3 STAT3 inhibits transcription of the inducible nitric oxide synthase gene by interacting with nuclear factor κB. *Biochem. J.* **367:** 97–105.

Yuan, Z.L., Guan, Y.J., Chatterjee, D., and Chin, Y.E. 2005. Stat3 dimerization regulated by reversible acetylation of a single lysine residue. *Science* **307:** 269–273.

Zhang, Z. and Fuller, G.M. 1997. The competitive binding of STAT3 and NF-κB on an overlapping DNA binding site. *Biochem. Biophys. Res. Commun.* **237:** 90–94.

Zhang, X., Wrzeszczynska, M.H., Horvath, C.M., and Darnell Jr., J.E. 1999. Interacting regions in Stat3 and c-Jun that participate in cooperative transcriptional activation. *Mol. Cell. Biol.* **19:** 7138–7146.

Zhong, H., Voll, R.E., and Ghosh, S. 1998. Phosphorylation of NF-κB p65 by PKA stimulates transcriptional activity by promoting a novel bivalent interaction with the coactivator CBP/p300. *Mol. Cell* **1:** 661–671.